

https://dspace.org/

Kinetics of the leaching of sphalerite in acidic ferric sulphate media in the presence and absence of oxygen

Crundwell, Frank Kenneth

2015-01-15
http://hdl.handle.net/10539/16555

Downloaded from a DSpace repository. https://dspace.org/

KINETICS OF THE LEACHING OF SPHALERITE IN ACIDIC FERRIC SULPHATE MEDIA IN THE PRESENCE AND ABSENCE OF OXYGEN.

Frank Kenneth Crundwell.

A dissertation submitted to the Faculty of Engineering, University of the Witwatersrand, Johannesburg, in fulfilment of the requirements for the degree of Master of Science in Engineering.

Johannesburg, 1985

DECLARATION.

I declare that this dissertation is my own, unaided work. It is being submitted for the Degree of Master of Science in Engineering in the University of the Witwatersrand, Johannesburg. It has not been submitted for any degree or examination in any other University.

Frank Cruickwell

17th day of September 1985.

ABSTRACT.

Sphalerite oxidation by Fe(III) in solution in the absence of oxygen was studied using two sphalerite concentrates:
(i) Black Mountain sphalerite forms an impervious product layer around the particle leaching to 40% conversion after 3 hours at 80°C in an excess of Fe(III). The passivation mechanism was shown by electromicrograph analysis not to be the formation of an insoluble lead sulphate layer. The initial rate is controlled by diffusion through the product layer.
(ii) Data obtained from the literature for the leaching of Gamsberg sphalerite is described by an electrochemical shrinking core model.

Oxidation of Fe(II) by oxygen was studied under different conditions of Fe(II) concentration, temperature, oxygen partial pressure and acid concentration, and a model, consistent with previously proposed models, was fitted to the data.

The leaching of Gamsberg sphalerite by Fe(III) in the presence of oxygen is well-described by the simultaneous numerical solution of the two equations which describe the models for leaching on its own and ferrous ion oxidation on its own. Leaching of Black Mountain sphalerite by Fe(III) in the presence of oxygen displayed the same passivation behaviour found without oxygen.

ACKNOWLEDGEMENTS.

I would like to thank the following people and institutions:

Dr. B. Verbaan, for his help and assistance;

Mr. D.F. Williams, for his help and encouragement;

The Council for Mineral Technology (MINTEK) for financing this project;

Dr. M.J. Dry, for arranging the mineralogical analysis at MINTEK.

CONTENTS.

	Page.
Declaration	i
Abstract	ii
Acknowledgements	iii
Contents	iv
List of figures	viii
List of tables	x
Nomenclature	xi
1. Introduction.	1.
1.1 Literature survey.	3.
1.1.1 Kinetics of sphalerite dissolution.	3.
1.1.2 Kinetics of the ferrous iron oxidation.	10.
1.2 Purpose and scope of this study.	13.
2. Theoretical analysis and modelling.	16.
2.1 Modelling of the sphalerite leach.	16.
2.1.1 Electrochemical model.	17.
2.1.2 Shrinking core behaviour.	26.
2.1.3 Electrochemical shrinking core model.	27.
2.2 Oxidation of ferrous iron by dissolved oxygen.	29.
2.3 Leaching of sphalerite in the presence of oxygen.	32.
3. Experimental procedure and results.	34.
3.1 Experimental reagents and analysis.	34.
3.1.1 Description of reagents.	34.

3.1.2 Methods of analysis. 36.
3.2 Apparatus. 36.
3.2.1 Large pressure reactor. 36.
3.2.2 Constant-temperature bath equipment. 38.
3.3 Experimental procedures. 39.
3.3.1 Procedure for leaching in the pressure reactor without oxygen present. 39.
3.2.2 Procedure for leaching in the constant-temperature bath reactor. 40.
3.3.3 Procedure for Fe(II) oxidation in the pressure reactor. 41.
3.3.4 Procedure for leaching in the pressure reactor with oxygen present. 41.
3.4 Experimental results. 42.
3.4.1 Results for sphalreite leaching without oxygen present. 42.
3.4.2 Experimental results for the oxidation of Fe(II) by oxygen. 47.
3.4.3 Experimental results for leaching with oxygen present. 48.

4. Analysis of expaimental leaching runs in the absence of oxygen. 51.
4.1 Leaching of Black Mountain sphalerite without oxygen. 51.
4.1.1 Leaching results for conditions of an excess ferric ion. 51.
4.1.2 Effect of agitation. 54.
4.1.3 Effect of temperature. 55.
4 1.4 Analysis of initial rates of leaching. 55.
4.2 Analysis of leaching data for Gamsberg sphalerite. 57.
4.3 Results for the mineralogical study, and discussion. 62.

5. Analysis of experimental Fe(II) oxidation results. 66.
5.1 Determination of the second order rate constant. 66.
5.2 Dependance of Fe(II) oxidation rate on hydrogen ion

concentration. 68.
5.3 Dependance of Fe(II) oxidation rate on temperature. 68.

6. Analysis of experimental leaching runs in the presence of oxygen. 71.
6.1 Analysis of leaching of Black Mountain sphalerite with oxygen present. 71.
6.2 Predicvion of Gamsberg leaching data with oxygen. 71.

7. Conclusions and recommendations. 74.

8. References. 77.

Appendix A. 82.
Equilibrium constants for the Fe(III)-Fe(II) sulphates complexing reactions.
Appendix B. 83.
Shrinking core model derivation, the reduction of Fe(III) ion by non-zinc sulphidic material, and the effect of the ZnO layer on the particle surface.
Appendix C. 88.
Values for corresponds given by Narita, Lawson and Han (1983).
Appendix D. 89.
Titration methods for Fe(III) and H_2SO_4 concentration determination.
Appendix E. 90.
Raw data for leaching of Black Mountain sphalerite without oxygen.
Appendix F. 97.

Raw data for the oxidation of ferrous ion by oxygen.
Appendix G. 101.
Raw data for Black Mountain sphalerite leaching with oxygen.
Appendix H. 102.
Experimental results for the determination of the oxide layers on th e surface of the sphalerite particles.
Appendix I. 104.
Analysis of Gamsberg leaching data in the absence of oxygen.
Appendix J. 107.
Estimation of parameters for the Fe(II) oxidation reaction.
Appendix K. 112.
FORTRAN 77 program for redox potential estimation, and the simulation of the leach rate.

LIST OF FIGURES.

Figure		page
2.1	Calculation of redox potential.	25.
3.1	Diagram of pressure leaching equipment.	37.
3.2	Diagram of constant temperature bath equipment.	37.
3.3	Leaching of sphalerite in an excess of Fe(III).	44.
3.4	Reproducibility of leaching results.	45.
3.5	Effect of agitation.	46.
3.6	Effect of Fe(III) and temperature.	46.
3.7	Typical results for the constant-temperature bath equipment.	47.
3.8	Fe(II) oxidation results.	48.
3.9	Leaching of sphalerite in the presence of oxygen	49.
3.10	Leaching of sphalerite in the presence of oxygen.	50.
4.1	Diffusion through product layer plot for runs 39, 40, and 42.	54.
4.2	Diffusion through product layer plot, indicating the effect of an increase in Fe(II), Fe(III) concentration, and agitation.	56.
4.3	Sum of squared differences surface Gamsberg leaching results.	59.
4.4	Equation 2.31 fitted to Gamsberg leaching data.	61.
4.5	Initial rate of leaching against the measured redox potential for Jamsberg sphalerite.	62.
4.6	The formation of $PbSO_4$ above the galena deposit.	63.
5.1	Second order plot for Fe(II) oxidation.	67.
5.2	Dependance of Fe(II) oxidation on H^+.	69.
5.3	Arrhenius plot for Fe(II) oxidation.	69.

6.1 Prediction of zinc extraction in the presence of oxygen. 72.
6.2 Prediction of iron changes in the presence of oxygen. 73.

I.1 Slice through sum of squares surface for constant k. 105.
I.2 Arrhenius diagram for G. sphalerite leaching results. 105.

J.1 Reproducibility of Fe(II) oxidation results. 109.

LIST OF TABLES.

Table		page
3.1	Particle size distribution for Black Mountain sphalerite.	35.
3.2	Chemical composition of Black Mountain sphalerite.	35.
4.1	Analysis of sphalerite leach residue.	53.
5.1	Comparison of Fe(II) oxidation kinetic expressions.	70.
I.1	Calculation of the minimum sum of squared errors for values of parameter k' for Gamsberg leaching data.	106.
I.2	Calculation of the dependance of rate on temperature for Gamsberg leaching data.	106.
J.1	Calculation of k, $[O_2]$, and $[H^+]$	108.
J.2	Dependance of Fe(II) oxidation on $[H^+]$	110.
J.3	Dependance of Fe(II) oxidation on temperature.	112.

NOMENCLATURE.

Symbol	Description	Units
a	Particle surface area, equ. 2.1	m^2
a(X)	Activity of specie X	-
A_s	Total initial surface for all paritcles equ 4.3	m^2
b	Parameter indicating Fe(II) dependance on $[H^+]$	-
C_i	Concentrations of dissolved specie i	M
E	Cell potential with respect to a reference cell, equ. 2.21	V
Eh	Solution redox potential, equ. 2.24	V
E_a	Activation energy	kJ/mol
$f(l_s)$	particle size distribution, equ. 2.30	-
F	Total mass particles	g
$F_{1-\alpha}$	F distribution, equ. 5.1	-
$\mathcal{F}$	Faraday's constant	J/Vmol
H	Henry's law constant, equ. 2.34	atm/mol
i	Partial current density, equ. 2.2	amps/m^2
k	Second order rate constant Fe(II) oxidation, equ. 5.1	l/Mmin
k_s	Fe(II) oxidation rate constant, equ. 2.33	
k_A, k_C	Anodic or cathodic rate constants	
k'	$(1-\beta_i)\mathcal{F}/RT$, section 5.2	
K	Leach rate constant, equ. 2.1	mol/m^2min
K_l	Solubility constant, equ. 2.36	l/M
l_s	Initial particle dimension	m
m	Amount of leachable material in a particle, equ. 2.3	mol
M	Total leachable material in all particles	mol
n	No. of model parameters, equ. 5.1	-
p	No. of data measurements, equ 5.1	-

$p(O_2)$	Partial pressure of oxygen	atm
r	Reaction rate, equ. 2.17	mol/m^2min
R	Gas constant	$J/^oKmol$
Rr	Minimum sum of squared errors, equ. 5.1	-
S	Solubility of oxygen in solution.	M
Ss	1-α confidence contour level, equ 5.1	-
t	Time	min
T	Temperature	^oK
X	Conversion of zinc or iron	-
[X]	Concentration of specie X	M
β	Symmetry factor, equ. 2.2	-
$\Delta\phi$	Mineral surface potential	V
$\Delta\phi^o$	Standard potential, activities are unity, equ. 2.20	V
γ	Shape factor, equ.2.27	-
ψ	Solutions conditions factor, equ. 2.1	-
ρ	mass density	g/m^2

1. INTRODUCTION.

Most modern commercial zinc plants employ a process consisting of a pyrometallurgical roasting step, followed by a hydrometallurgical leach step to convert sphalerite, a zinc sulphide mineral, to zinc in solution and sulphur dioxide. The zinc in solution is subsequently electrowon. The sulphur dioxide is either released to the atmosphere, or converted to sulphuric acid in an acid plant. Van Niekerk and Allen (1977) describe a typical roast-leach zinc process. A substantial proportion of the plant capital cost is attributed to the acid plant, and much of the running costs are due to the roasting step.

Alternative technologies, consisting only of hydrometallurgical steps which produce elemental sulphur, have been developed by Sherritt-Gordon Mines, Ltd., and the Council for Mineral Technology (MINTEK). These alternatives have the advantage that they do not require an acid plant, since they produce elemental sulphur which is more easily stored and transported than sulphuric acid, and that lower ore grades can be treated more easily.

Doyle, Masters, Webster and Veltman (1978) compared the roast-leach with an alternative hydrometallurgical process, and reported on the research and development done on direct pressure leaching technology at Sherritt-Gordon Mines, Ltd.. Zinc sulphide concentrate is leached in cell-house return acid with an over-pressure of oxygen according to:

$$ZnS + H_2SO_4 + 1/2\ O_2 \rightarrow ZnSO_4 + H_2O + S^o \qquad 1.1$$

in a pressure leach vessel at temperatures above the melting point of sulphur, 160°C. Surface active agents are added to ensure complete conversion in a single or two-stage autoclave configuration.

Verbaan (1981) patented a process developed at MINTEK in which zinc sulphide material is leached below the melting point of sulphur, 119°C, in a two step process. The zinc is dissolved in a solution containing 5 to 50 g/l iron and a maximum of 20 g/l sulphuric acid from cell-house return acid. The main difference between this and the Sherritt-Gordon process are the conditions under which leaching occurs, and that in the MINTEK process the iron is partially oxidised in a separate operation to the dissolution.

In both the Sherritt-Gordon and the MINTEK processes the sphalerite flotation concentrate is leached under pressure in an acidic ferric sulphate medium. The solution contains sulphuric acid, dissolved oxygen, ferric ions, ferrous ions and zinc ions. A fundamental understanding of the process would aid in both the design and operation of plants employing these, or similar technologies.

The remaining portion of chapter 1 outlines the research that has been done in the area of modelling the sphalerite dissolution mechanism, and then defining the purpose and scope of this study. Research on the oxidation of ferrous ion by dissolved oxygen is also reviewed. In chapter 2 a mathematical model describing the rate-limiting step of the sphalerite dissolution as an electrochemical reaction is derived and a model describing the ferrous ion oxidation reaction based on the work of previous researchers is also presented. The experimental work is reported in chapter 3. The experimental results for the leaching of sphalerite from the Black Mountain and ore deposits are analysed in chapter 4. Data for the leaching of Black Mountain sphalerite was measured in this study,

while that for the Gamsberg sphalerite was obtained from the literature (Verbaan, 1980). The ferrous ion oxidation results are analysed in chapter 5, while the results for the combined system, that is, the leaching of sphalerite from Black Mountain and Gamsberg ore deposits in acidic ferric sulphate media in the presence of oxygen, are analysed in chapter 6. Again, the data for Black Mountain leaching was measured in this study while that for the Gamsberg was taken from the literature. The conclusions and recommendations are discussed in chapter 7.

1.1 Literature survey.

The pressure leaching of the sphalerite in acidic ferric sulphate solution in the presence of dissolved oxygen is a three-phase system. It consists of solid sphalerite, acidic ferric sulphate in solution and oxygen in gaseous and dissolved forms in a stirre[illegible]r. The sphalerite leach reaction consumes ferric ion, and produ[illegible]s ion, zinc in solution, and elemental sulphur. The dissolved oxy[illegible]dises the ferrous ion to the ferric state. If it is assumed that these two reactions occur independently of each other, then they can be treated separately.

1.1.1 Kinetics of sphalerite dissolution.

Forward and Warren (1960) reviewed the available literature for the extraction of metals from base metal sulphides by hydrometallurgical methods and reported on the chemistry of the dissolution process. They concluded that the products of the reaction are largely determined by the hydrogen ion concentration, the presence or absence of an oxidising agent,

and the temperature in so far as it affects the formation of sulphates. In the absence of an oxidising agent, the reaction is:

$$ZnS + H_2SO_4 \rightarrow ZnSO_4 + H_2S \qquad 1.2$$

while in the presence of oxygen, the reaction is:

$$ZnS + H_2SO_4 + 1/2\ O_2 \rightarrow ZnSO_4 + H_2O + S^\circ \qquad 1.3$$

Oxidation by oxygen can occur directly in solutions of higher pH values, as follows:

$$ZnS + 2O_2 \rightarrow ZnSO_4 \qquad 1.4$$

In the presence of ferric ion as an oxidising agent, the overall dissolution reaction occurs as follows:

$$ZnS + Fe_2(SO_4)_3 \rightarrow ZnSO_4 + 2FeSO_4 + S^\circ \qquad 1.5$$

This reaction may occur with hydrogen sulphide as an intermediate, or by direct oxidation. Scott and Nicol (1978) distinguished between an oxidative reaction, in which the sulphide sulphur is oxidised directly in the dissolution step, and a non-oxidative reaction, in which the sulphide sulphur is oxidised in a subsequent reaction. This can be illustrated as follows:

Oxidative dissolution.

$$ZnS + Fe_2(SO_4)_3 \rightarrow ZnSO_4 + 2FeSO_4 + S^\circ \qquad 1.6$$

Non-oxidative dissolution.

$$ZnS + H_2SO_4 \rightarrow ZnSO_4 + H_2S \qquad 1.7\ a$$

$$H_2S + Fe_2(SO_4)_3 \rightarrow H_2SO_4 + 2FeSO_4 + S^\circ \qquad 1.7\ b$$

The dominant dissolution mechanism would depend on the relative concentration of ferric ion and sulphuric acid. In a solution of high ferric ion concentration, oxidative dissolution would be expected to occur, while in a solution of high acidity the non-oxidative process will dominate.

Forward and Warren (1960) separated the factors that may control the rate of dissolution of sulphide minerals into three categories: (i) Mass transfer of reactants or products in the solution, (ii) Coating of insoluble products on the surface of the mineral, or (iii) Chemical reaction on the surface of the mineral, or in the solution. They reported that when oxidation occurs below 118°C, the film of elemental sulphur that is formed is porous, and does not inhibit oxidation. Between 118°C and 160°C, the sulphur coats the mineral and prevents further oxidation, while above 160°C the sulphur oxidises completely to sulphate, and, therefore, does not inhibit the dissolution.

Woodcock (1961) reviewed the literature published prior to 1961, and reported cases where each of the above-mentioned rate-controlling mechanisms occur. He also reported that the reaction at the surface was electrochemically controlled, and suggested that more work be done in that area.

Dutrizac and Macdonald (1974) reviewed the literature for the leaching of base metal sulphides by ferric ion and reported that the leaching of sphalerite is controlled by the diffusion of ferric iron in solution, with an activation energy of about 24 kJ/mol, which is consistent with diffusion control. It was also also reported that the rate is directly proportional to the ferric ion concentration, and is not impeded by the formation of elemental sulphur.

Rath, Paramguru and Jens (1981) reported an activation energy of about 90 kJ/mol for the leaching of a synthetic zinc sulphide in acidic ferric chloride media. This value is too high for liquid film diffusion control. They obtained parabolic kinetics, and proposed that the rate is controlled by ferric ion diffusion through the elemental sulphur layer.

Jan, Hepworth and Fox (1976) concluded that the rate determining step was the reaction at the mineral surface, and not ferric ion diffusion, even though he observed an apparent activation energy of 24 kJ/mol, and a dependance on agitation. they attributed the linear kinetics that he obtained to the shape of the sphalerite particles which appeared to have a disk-like shape when examined under an electron-microscope. In the absence of an oxidising agent other than oxygen, he proposed that the reaction proceeds according to equation 1.7, that is, non-oxidatively. By leaching ZnS in the presence of sulphuric acid and iodide, he demonstrated that the reaction:

$$ZnS + H_2SO_4 \rightarrow ZnSO_4 + H_2S \qquad 1.8$$

was instantaneous, and that oxidation of hydrogen sulphide by oxygen:

$$H_2S + 1/2O_2 \rightarrow H_2O + S^o \qquad 1.9$$

is slow and rate determining. In the presence of ferric ion, he proposed that the role of the oxygen is to re-oxidise the ferrous ion produced in oxidising the hydrogen sulphide. This scheme can be represented by:

$$ZnS + H_2SO_4 = ZnSO_4 + H_2S \qquad 1.10\ a$$

$$2FeSO_4 + H_2SO_4 + {}^{1}/_{2}\ O_2 \rightarrow Fe_2(SO_4)_3 + H_2O \qquad 1.10\ b$$

$$Fe_2(SO_4)_3 + H_2S = 2FeSO_4 + H_2SO_4 + S^o \qquad 1.10\ c$$

and the overall reaction would then be:

$$ZnS + H_2SO_4 + 1/2\ O_2 \rightarrow ZnSO_4 + H_2O + S^o \qquad 1.10\ d$$

with reaction 1.10c as the rate-determining step.

Verbaan (1977) leached a number of different types of sphalerites in the presence and absence of ferric ion in acid sulphate media. He attempted to explain the mechanism of dissolution in terms of Langmuir-Hinschelwood adsorption isotherms, and was relatively successful in the absence of ferric ion. He showed that the H_2S formed during reaction was dramatically decreased by the addition of ferric ion. He obtained conflicting evidence as to whether or not the elemental sulphur resulted in product-layer diffusion control.

Pawlek (1969) proposed an entirely different mechanism for the pressure leaching of zinc blende in the presence of dissolved oxygen. He described the kinetics in terms of an electrochemical model, analogous to the corrosion of metals. This description involves anodic and cathodic partial reactions occurring on the surface of the mineral, with a current flowing between the localities where the separate partial reactions take place. The anodic partial reaction releases electrons by:

$$ZnS \rightarrow Zn^{2+} + S^o + 2e^- \qquad 1.11$$

while the cathodic reaction consumes the electrons produced by:

$$2e^- + 2H^+ + 1/2\ O_2 \rightarrow H_2O \qquad 1.12$$

Although zinc blende is a semi-conductor with a very high resistivity

(6×10^{9} [illegible] cm), the electron exchange occurs over a limited locality and the high [illegible]sistance of the mineral does not limit the electrochemical reaction. In a study of the electrochemical behaviour of various samples of galena (PbS), Sprenger (1970) concluded that the electronic conduction properties of minerals do not normally affect the oxidation and dissolution reactions in which electrochemical reactions are important.

Pawlek (1969) did not describe the overall kinetics in terms of an electrochemical model alone, but used a theory of boundary chemisorption, indicating that other rate controlling processes are involved. He found that initial dissolution resulted in the formation of H_2S which retards the dissolution. Pawlek showed experimentally that continuous removal of H_2S can increase the rate of dissolution by approximately 4 times.

Scott and Nicol (1978) reported inconsistencies between the experimental observations and the predictions based on the assumption that the dissolution occurs by means of a non-oxidative attack for various different sphalerites and suggested that the mechanism of dissolution in acidic ferric sulphate media might be direct oxidation. They concluded that the mechanism of dissolution is dependant on the type of sphalerite. Using a sphalerite-graphite electrode they indicated that the process directly responsible for the rate of dissolution occurs on the surface of the electrode, and that if direct oxidation does occur one would expect the potential of the zinc sulphide surface to lie in the region of +0,4 V with reference to the standard calomel electrode. They experienced difficulty with this type of experiment due to the high resistivity of sphalerite. In addition, they suggested that the sulphur produced at the surface may retard the non-oxidative dissolution.

Scott and Dyson (1968) noted the catalytic activity of several metals on the oxygen pressure leaching of a chemically prepared zinc sulphide. This

activity increased in the order Fe < Mo < Ru < Bi < Cu. The effect of the catalysts was attributed to penetration that influences the electronic conductivity of the lattice, and thus allowing electrochemical dissolution to occur according to equation 1.11 at the solid surface. The main parameters affecting dissolution were catalyst concentration, temperature, oxygen pressure and acid concentration. The sulphate that formed was attributed to the oxidation of H_2S, that formed as an intermediate product.

Wadsworth (1972) reviewed the literature for the leaching of base metal sulphides. He presented a generalised rate expression for the dissolution mechanism containing diffusion, chemical reaction, and electrochemical reaction terms. In order to evaluate the influence of the potential on the kinetics, an electrode was made from chalcopyrite and the potential was measured. He concluded from his results that cathodic reduction of oxygen at the surface controlled the electrochemical kinetics. He stated that the large activation energy and parabolic kinetics suggested diffusion through the product layers controlled dissolution. He concluded that the role of the electrochemical reaction is not clear from the observed kinetics for chalcopyrite.

Verbaan (1980) concluded in a later examination that the kinetics of the leaching of sphalerite is electrochemical in nature in which the rate is dependant on the ratio of the ferric ion concentration to the power 0,4 to the ferrous ion concentration to the power 0,25, and reported an empirical correlation based on this for the leaching results in acidic ferric sulphate media. No attempt was made to use electrochemical theory in the formulation of this correlation.

Dry (1984) reviewed the literature for base metal sulphides. He leached low grade matte in acidic ferric sulphate media, and proposed that the

mechanism of dissolution is electrochemically controlled. He presented an electrochemical model incorporating the prediction of the redox potential as an approximation for the mineral surface potential. (This model will be discussed in greater depth in chapter 2.) He incorporated the kinetics proposed for anodic dissolution of galena (PbS) by Paul, Nicol, Diggle and Saunders (1977), who proposed that galena dissolves anodically in two single-electron transfer steps via S^- as an intermediate to explain the results they obtained from a PbS electrode using cyclic voltammetry.

It appears that the more recent studies for sphalerite, and other sulphide minerals, favour the proposition that the leach dissolution reaction is electrochemical in nature. However, every general category of rate-controlling mechanism has been proposed. The type of rate-controlling step appears to be dependant on the composition of the particular sphalerite.

1.1.2 Kinetics of the ferrous ion oxidation reaction in sulphate media.

Huffman and Davidson (1956) proposed that the overall reaction:

$$4Fe^{2+} + O_2 + 4H^+ \rightarrow 4Fe^{3+} + 2H_2O \qquad 1.14$$

proceeds by simultaneous bimolecular and trimolecular reaction paths described by:

$$-\frac{d[Fe(II)]}{dt} = k_b[Fe(II)]p(O_2) + k_t[Fe(II)]^2p(O_2) \qquad 1.15$$

where k_b and k_t are the reaction rate constants for the bimolecular and trimolecular reactions. They observed that the rate decreases with in-

creasing hydrogen ion concentration, but made no attempt to incorporate this in their rate equation. Mention is also made of the catalytic effect of the Cu^{2+} ion.

Using a gas lift percolator for their experimental work, Mathews and Robins (1972) proposed a rate equation of the form:

$$-\frac{d[Fe(III)]}{dt} = k_o\,[Fe(II)]^{1,84}[O_2]\,/[H^+]^{0,25}\,\exp(-73,9/RT)\quad 1.16$$

where k_o is the overall reaction rate constant. The presence of Cu^{2+} was found to increase the rate of oxidation while the effect of Ni, Zn, Co, Hg, Cl, Mo, NH_4^+, As, Cr, and Na at a concentration of 0.001 M in 0.2 M Fe(II) was found to be negligible. The concentration of Fe(III) was measured spectrophotometrically and the H^+ concentration was estimated from pH measurements at ambient temperature. They determined the oxygen concentration from:

$$[O_2] = [O_2]_{sat} - k_m/k_o \qquad 1.17$$

where k_m and k_o are the rate constants for the oxygen dissolution reaction and the ferrous oxidation reaction respectively. The rate constant k_m was measured without any iron in solution at the correct pH and temperature by measuring the dissolved oxygen concentration using an oxygen electrode. No correction was made for the reduced solubility of the oxygen as a result of the other solutes present. Subsequent experiments were made at a sufficiently high gas flowrate so that it would not affect the value of k_m.

Nicol (1975) confirmed the results of Mathews and Robins (1972) in terms of the dependance of the rate on ferrous ion and oxygen partial pressure, but made no attempt to quantify the role of the hydrogen ion. He con-

sidered the effect of total concentration of dissolved electrolyte, and operated his experiments at a gas flowrate sufficiently large to allow the concentration of dissolved oxygen to approach the saturation concentration at that temperature and oxygen partial pressure. The saturation concentration of dissolved oxygen experiences a 'salting out' effect, in which the solubility of oxygen decreases exponentially with increasing electrolyte concentration. Nicol found that the second order rate constant, k, given by:

$$\frac{d[Fe(III)]}{dt} = k[Fe(II)]^2 \qquad 1.18$$

was described by the empirical fit:

$$k = 0{,}0476\, p(O_2)\exp(-0{,}0056 C_e) \qquad 1.19$$

where C_e is the total concentration of dissolved electrolyte ($g\ l^{-1}$) He also did a number of experiments at a low gas flowrate where the mass-transfer of oxygen to the solution is the controlling mechanism. He determined the mass-transfer coefficient, and discussed the effect of temperature and total concentration of dissolved electrolyte on it.

Iwai, Majima, and Awakwa (1982) studied the oxidation of Fe(II) with dissolved molecular oxygen in sulphuric acid solutions using a glass autoclave. They, too, suggest that the reaction occurs in two paths according to:

$$-\frac{d[Fe(II)]}{dt} = A_o[Fe^{2+}]^2\, p(O_2)\exp(-51{,}6/RT) + A_1[SO_4^{2-}][Fe^{2+}]^2 p(O_2)\exp(-144{,}0/RT) \qquad 1.20$$

where A_o and A_1 represent the reaction rate constants of the two reaction paths. They accounted for the following species in solution: $FeSO_4$,

$FeHSO_4^+$, HSO_4^-. Their work seemed to indicate that the role of the hydrogen ion is contradictory and made no attempt in their formulation of the rate equation to quantify it. Instead, they attributed this behaviour apparantly due to the hydrogen ion, to the sulphate ion and included that in their rate equation. They observed a deviation from second order kinetics for Fe(II) in some runs and attributed this to the sulphate ion as well.

Chmielewski and Charewicz (1984) presented second order kinetics with respect to Fe(II) concentration and first order kinetics with respect to oxygen partial pressure with an activation energy of 56,9 kJ/mol°K, provided the ferrous ion concentration did not exceed 3-8 g/l. They observed a deviation from second order kinetics at higher conversions and proposed that under those conditions the reaction kinetics are first order with respect to the ferrous ion concentration. Since only the higher ferrous ion concentration region was of technological importance to them, they did not quantify the low Fe(II) concentration kinetics.

The kinetics of the ferrous ion oxidation reaction shows some discrepancy between the proposals of the various researchers. However, the consensus appears to be that the rate is second order in ferrous ion concentration, at least in the initial stages of the reaction, and first order in oxygen concentration. The rate is inversely proportional to a power of the hydrogen ion concentration.

1.2 Purpose and scope of this study.

The review of the literature indicates that the sphalerite dissolution reaction may be controlled by many different mechanisms. However, the

proposition that the reaction is electrochemical in nature cannot be tested directly by making a sphalerite electrode and measuring the electrochemical current since the resistivity of sphalerite is so high that very little current flows, and the potential difference across the sphalerite electrode swamps the applied potential difference (Scott and Nicol, 1978). A rate equation describing the leaching of sphalerite by ferric ion incorporating electrochemical kinetics has, as yet, not been proposed and tested. It is the purpose of this study to do so.

The aims of the present study are:

(i) to describe the kinetics of two natural sphalerites leaching under conditions of oxidation by ferric ion in the absence of oxygen by a fundamental model based on an electrochemical mechanism, and to test this model for experimental data reported in the literature, and obtained in this study;

(ii) to describe the overall kinetics of the ferrous ion oxidation reaction by dissolved oxygen as second order in Fe(II) and first order in oxygen concentration and dependant on a power of the hydrogen ion concentration, and to fit this model to data obtained in this study;

(iii) to model the kinetics of sphalerite dissolution in the presence of dissolved oxygen in acidic ferric sulphate media as the simultaneous solution of the kinetic equations for (i) and (ii) above, and to test this model for experimental data reported in the literature, and obtained in this study.

The propositions of this study are that leaching occurring within the scope of this work occurs primarily by an electrochemical oxidative attack, and that the role of the oxygen reaction is to oxidise the ferrous ion in solution.

The present study is restricted to the region where:

(i) The leaching of sphalerite is confined to acid concentrations where little or no H_2S is formed, that is, where leaching occurs by direct oxidation, generally below concentrations of 0,25 M H_2SO_4 (refer to Nicol and Scott, 1978 and Verbaan, 1977).

(ii) Ferric ion is stable in acidic sulphate solutions at pH values below 2. Since the study is concerned with leaching due to ferric ion, the acid concentrations must remain in this region. to prevent precipitation of ferric ions. (Refer to McAndrew, Wang, and Brown, 1975).

(iii) The ferrous ion oxidation reaction is confined to region where the oxygen partial pressure is below 500 kPa gauge,

(iv) and the stirrer speed is such that the mass-transfer of oxygen from the gaseous phase to the aqueous phase is rapid, and not rate-limiting.

2. THEORETICAL ANALYSIS AND MODELLING.

The work of Jan, Hepworth and Fox (1976) indicates that the role of oxygen in the pressure leaching of sphalerite in ferric sulphate media is to oxidise the ferrous species in solution, and that oxygen does not contribute to the dissolution reaction occurring at the mineral surface. Wadsworth (1972) reports that at the mineral surface, in the absence of any iron species, the oxygen reacts to form intermediates, such as H_2O_2 and HO_2, in a series of single electron charge transfer processes, resulting in a relatively slow discharge of oxygen due to the strength of the oxygen-oxygen double bond. Therefore, even though the presence of oxygen may act as an oxidant in addition to the effect of ferric ion, the partial current due to this reaction is likely to be small since the rate of this reaction is slow, and can be neglected.

Assuming that the leach reaction and the ferrous oxidation reaction occur independently of one another, the oxidative leach in the presence of oxygen can be modelled as the simultaneous solution of the two rate equations describing each separate reaction.

2.1 Modelling of the sphalerite leaching kinetics.

The leaching of a single sphalerite particle occurs at the particle surface, producing a porous sulphur layer as the reaction proceeds. This 'shrinking core' process (refer to Levenspiel, 1971) is represented by:

$$\frac{dm}{dt} = - K a \psi \qquad 2.1$$

where m = amount of leachable metal remaining in the core (mol);
s = particle surface area available for leaching (m^2);
ψ = factor depending on the conditions within the solution (-);
K = rate constant ($mol/m^2 min$).

The essential part of the formulation of the model describing the dissolution is contained in determining the way in which the area changes during dissolution and the effects that constitute the solution conditions factor, ψ. The solution conditions factor is determined by the electrochemical model, and the effect of area changes is described by the shrinking core model.

2.1.1 Electrochemical model.

The dissolution of a particle by electrochemical attack is described in a way that is analogous to the electrochemical corrosion mechanism. Two partial reactions occur at separate localities on the surface of the particle: an anodic reaction supplies electrons by $D \rightarrow A^+ + e^-$, and a cathodic reaction consumes electrons by $A^+ + e^- \rightarrow D$. In corrosion and leaching the anodic reaction would be the dissolution reaction and the cathodic reaction would be a reaction in which an oxidant in the solution would consume the electrons supplied by the dissolution. Since there cannot be any net current flowing, as the particle is a closed surface, the current produced and consumed by both partial reactions must be the same. The Butler-Volmer equation describes the electrochemical kinetics in terms of the anodic current density, i_A and the cathodic current density, i_C. Refer to Bockris and Raddy (1970) for a thorough treatment of electrochemical phenomena. For the anodic reaction the current density is:

$$i_A = \mathcal{F} k_A [D] \exp((1-\beta)\Delta\phi\mathcal{F}/RT) \qquad 2.2$$

and for the cathodic reaction this is:

$$i_C = \mathcal{F} k_C [A^+] \exp(-\beta\Delta\phi\mathcal{F}/RT) \qquad 2.3$$

where β = symmetry factor (-);
$\Delta\phi$ = potential difference across the Helmholtz plane at the mineral surface (V);
[D] = concentration or activity of species D (mol/l);
$\mathcal{F}$ = Faraday's constant (J/V mol);
k = rate constant;
T = temperature (°K);
R = gas constant (J/°K mol).

The subscripts A and C refer to the anodic and cathodic partial reactions respectively. The potential, $\Delta\phi$, is the difference between the electrical potential of the solution, $\phi(S)$, and that of the mineral surface, $\phi(M)$, where S and M represent the solution and mineral respectively. To measure this another cell has to be in series with this, and the measured potential difference with respect to this reference cell is denoted E.

Paul, Nicol, Diggle and Saunders (1977) studied the electrochemical behaviour of the dissolution of galena (PbS), and derived an electrochemical model based on this mechanism which successfully predicted their results:

Representing the metal sulphide as MS, this kinetic model can be represented as:

1) $MS = M^{2+} + S^- + e^-$ 2.4 a

2) $S^- \rightarrow S^o + e^-$ 2.4 b

Applying the approximation that the rate of formation of the low concentration intermediate, 'S^-', is equal to the rate of consumption, then:

$$0 = i_{1A} - i_{1C} - i_{2A} \qquad 2.5$$

where A represents anodic and C cathodic, and 1 represents reaction 1, and 2 reaction 2. Writing the Butler-Volmer equation for each of these partial electrode reactions:

$$0 = k_{1A}[MS]\exp((1-\beta_1)\Delta\phi\mathcal{F}/RT) - k_{1C}[M^{2+}][S^-]\exp(-\beta_1\Delta\phi\mathcal{F}/RT) - k_{2A}[S^-]\exp((1-\beta_2)\Delta\phi\mathcal{F}/RT) \qquad 2.6$$

The subscripts of the symmetry factors refer to reactions 1 and 2, that is, equations 2.4 a and b.

The overall anodic current is $i_A = 2i_{2A}$, that is,

$$i_A = 2k_{2A}\mathcal{F}[S^-]\exp((1-\beta_2)\Delta\phi\mathcal{F}/RT) \qquad 2.7$$

Eliminating $[S^-]$ from equations 2.6 and 2.7 gives:

$$i_A = 2\mathcal{F}k_{1A}k_{2A}\exp((2-\beta_1-\beta_2)\Delta\phi\mathcal{F}/RT)/\Sigma i \qquad 2.8$$

where $\Sigma i = k_{1C}[M^{2+}]\exp(-\beta_1\Delta\phi\mathcal{F}/RT) + k_{2A}\exp((1-\beta_2)\Delta\phi\mathcal{F}/RT)$

Assuming that the potential for reaction 1 is large relative to the equilibrium potential, so that the first term of the denominator of i_A is small, the anodic dissolution current reduces to:

$$i_A = 2\mathcal{F}k_{1A}\exp((1-\beta_1)\Delta\phi\mathcal{F}/RT) \qquad 2.9$$

For the ferrous-ferric couple,

3) $Fe^{3+} + e^- = Fe^{2+}$ 2.10

the current is given by:

$$i_{Fe} = \mathcal{F}k_{3A}[Fe^{2+}]\exp((1-\beta_{3_1})\Delta\phi\mathcal{F}/RT) - \mathcal{F}k_{3C}[Fe^{3+}]\exp(-\beta_{3_2}\Delta\phi\mathcal{F}/RT) \quad 2.11$$

where β_{3_1} represents the symmetry factor for the anodic reaction of equation 2.10, and β_{3_2} the cathodic reaction.

Since no net current flows during leaching,

$$0 = i_A + i_{Fe} \quad 2.12$$

Re-arranging and simplifying, the following expression is obtained:

$$0 = 2k_{1A}\exp((1-\beta_1)\Delta\phi\mathcal{F}/RT) + k_{3A}[Fe^{2+}]\exp((1-\beta_{3_1})\Delta\phi\mathcal{F}/RT) - k_{3C}[Fe^{3+}]\exp((-\beta_{3_2})\Delta\phi\mathcal{F}/RT) \quad 2.13$$

Nicol, Needles and Finkelstein (1975) showed that the role of the iron couple can be divided into 3 regions:

(i) The partial anodic current due to the oxidation of Fe^{2+} is negligible.

(ii) The partial anodic currents due to the oxidation of Fe^{2+} and ZnS are significant.

(iii) The partial anodic current due to the oxidation of ZnS is negligible compared with that due to the oxidation of Fe^{2+}.

The equations describing these 3 cases are derived by solving equation 2.13 for exp(Δφ/RT) and substituting this in equation 2.9. They are as follows:

Case (i)

$$i_A = \mathcal{F}\ (2k_{1A})^{\alpha}\ (k_{3C}\ [Fe^{3+}])^{\delta} \qquad 2.14$$

where $\alpha = \beta_{32}/(1-\beta_1+\beta_{32})$ and $\delta = (1-\beta_1)/(1-\beta_1+\beta_{32})$

Case (ii)

$$i_A = 2\mathcal{F}k_{1A}\ (k_{3C}[Fe^{3+}]\ /(2k_{1A} + k_{3A}[Fe^{2+}]))^{0,5} \qquad 2.15$$

case(ii) assumes that the β values are equal.

Case (iii)

$$i_A = 2\mathcal{F}k_{1A}\ (k_{3C}[Fe^{3+}]/k_{3A}[Fe^{2+}])^{\delta} \qquad 2.16$$

where $\delta = (1-\beta_1)/(1-\beta_1+\beta_{32})$

These three cases can be expressed in the generalised form:

$$i_A = 2\mathcal{F}k_{1A}(k_{3C}[Fe^{3+}]/(\ 2k_{1A} + k_{3A}[Fe^{2+}]))^{\delta} \qquad 2.17$$

where δ = a parameter dependant on the symmetry factors.

An equivalent statement to that of equation 2.12, that is, that the net current density is zero, is that the reaction occurs at the mixed potential, $\Delta\phi_m$, that satisfies the thermodynamic equilibrium conditions which

occur when the current density is zero. The overall dissolution reaction is:

$$ZnS + 2Fe^{3+} \rightarrow Zn^{2+} + S^{o} + 2Fe^{2+} \qquad 2.18$$

and the mixed potential, $\Delta\phi_m$ is:

$$\Delta\phi_m = \Delta\phi^{o} + RT/2\mathcal{F} \ln (\text{activity ratio}) \qquad 2.19$$

$$\text{activity ratio} = [\ a(Fe^{3+})^2\ a(ZnS) / [\ a(Fe^{2+})^2 a(Zn^{2+})\ a(S^{o})\ ]]$$

where $a(X)$ = activity of species X

$\Delta\phi^{o}$ = standard potential for reaction 2.18.

The standard potential is that when the activities are unity. Since ZnS and S^{o} are solids their activities are unity:

$$\Delta\phi_m = \Delta\phi^{o} + RT/2\mathcal{F} \ln [\ a(Fe^{3+})^2 / [\ a(Fe^{2+})^2 a(Zn^{2+})\ ]] \qquad 2.20$$

Case (i) conditions are described when $a(Fe^{2+})$ is close to unity, and case (iii) conditions occur when $a(Zn^{2+})$ is close to unity. Therefore, if the activities of the various species could be accurately predicted, then this prediction of the mixed potential could be substituted directly into equation 2.9 (the mineral surface potential is the mixed potential), to describe the leach kinetics. Since $\Delta\phi^{o}$ cannot be determined on its own, but only with respect to another cell, normally the standard hydrogen electrode, the potential that is substituted into equation 2.9 is:

$$E_m = E^{o} + RT/2\mathcal{F} \ln [\ a(Fe^{3+})^2 / [\ a(Fe^{2+})^2 a(Zn^{2+})\ ]] \qquad 2.21$$

where E_m is the mixed potential with reference to the standard hydrogen electrode. E^{o} is the standard potential for equation 2.19 and can be calculated from the standard Gibbs free energy for the reaction. It has a value of 0,5061 V, calculated from the values given by Latimer (1952).

Dry (1984) leached low-grade mattes in acidic ferric sulphate media, and observed that the redox potential measured with a platinum electrode followed the extent of reaction, and when used as an approximation for the surface potential difference, $\Delta\phi$, successfully predicted his leaching results. Approximating $\Delta\phi$ in equation 2.9 by the redox potential, Eh, given by:

$$Eh = E^{\circ} + RT/\mathcal{F} \ln [\ a(Fe^{3+})/a(Fe^{2+})\ ] \qquad 2.22$$

where $a(Fe^{2+})$ and $a(Fe^{3+})$ are the activities of the ferrous and ferric ion species respectively, and E° is the standard potential vs S.H.E. for the ferrous-ferric half reaction (the standard state is that when the activities are unity). The value of E° given by Yeager and Salkind (1972) is 0,771 + 0,00119(T-298).

This is essentially the same as case (iii) conditions, that is, assuming that the partial anodic current due to leaching is negligible compared to that of the oxidation of the ferrous ion. The activities of the ferrous and ferric species in solution are affected by the presence of any ferrous or ferric sulphate complexes formed. Ferric ion is stable in aqueous sulphate solutions with pH values below approximately 2; in this region the following equilibria involving ferrous and ferric ion are significant:

$$Fe^{3+} + H^{+} + 2SO_4^{2-} = FeHSO_4SO_4 \qquad 2.23\ a$$

$$Fe^{3+} + H^{+} + SO_4^{2-} = FeHSO_4^{2+} \qquad 2.23\ b$$

$$Fe^{3+} + H^{+} + SO_4^{2-} = Fe(SO_4)_2^{-} \qquad 2.23\ c$$

$$Fe^{3+} + SO_4^{2-} = FeSO_4^{+} \qquad 2.23\ d$$

$$F^{+} + SO_4^{2-} = HSO_4^{-} \qquad 2.23\ e$$

$$Fe^{2+} + SO_4^{2-} = FeSO_4 \qquad 2.23\ f$$

$$Fe^{2+} + H^{+} + SO_4^{2-} = FeHSO_4^{+} \qquad 2.23\ g$$

The presence of zinc in solution adds the equilibrium:

$$Zn^{2+} + SO_4^{2-} = ZnSO_4 \qquad 2.23\ h$$

These complexes are be described by the total concentrations of the following components Fe^{3+}, Fe^{2+}, H^+, SO_4^{2-}, and Zn^{2+} and the equilibrium constants. Refer to Appendix A for the equilibrium constants. The total concentration of each component must remain constant at equilibrium, and a mass balance is written for each of the components. The concentrations of the complexes are expressed in terms of the concentrations of the components, the equilibrium constants and the activity coefficients. The activity coefficients are evaluated by the Debye-Huckel equation (Kortum, 1965). This results in five simultaneous non-linear equations in five variables, the concentrations of the five components. These equations are solved using a iterative Newton-Raphson technique. Ting-Po and Narcollas (1972) discuss a quadratic search in the direction given by the Newton-Raphson solution at each iteration that speeds convergence.

The subprogram EQUIL has been written in FORTRAN 77 to perform this calculation, and is listed in Appendix K. Figure 2.1 represents the predicted and calculated redox potentials plotted against the log of the ratio of the ferric ion activity to the ferrous ion activity. The measured values are the points on the graph and are from Dry (1984), and the line represents the calculated values from the subprogram EQUIL. The liquid junction potential has been accounted for by the Henderson equation (Kortum, 1965) in the subprogram EQUIL. There is good agreement between the measured and the calculated values, and the values calculated from this subprogram are substituted for the redox potential with a high degree of confidence.

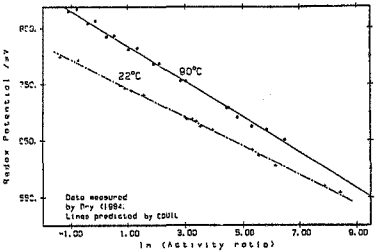

Figure 2.1 Calculation of redox potential. Data points measured by Dry (1984) and lines represent the calculations of the subprogram EQUIL to predict Eh. Activity ratio is the ratio of activities of ferric to ferrous ion.

This prediction of the the redox potential of the solution, Eh, is substituted for $\Delta\phi$ in equation 2.9, and since the rate of reaction is expressed in terms of Faraday's law, that is,

$$r = -\frac{1}{a}\frac{dm}{dt} = \frac{i_A}{2F} \qquad 2.24$$

then

$$\frac{1}{a}\frac{dm}{dt} = -K\exp((1-\beta_1)Eh\bar{F}/RT) \qquad 2.25$$

is used to simulate the leaching results. Note that K and k_{1A} are identical in this case.

2.1.2 Shrinking core behaviour

The effect of the change in area of the particle is modelled by the shrinking core model (refer to Loveday, 1975). By defining the characteristic particle size, l, as: l^3 = volume of the particle, the surface area, a, in terms of the shape factor, γ, as: $a = \gamma l^2$, and the molar density as: $m_0/l_0^3 = m/l^3$ where m_0 and l_0 are the values of m and l at the beginning of the leach, that is, at t=0, and rearranging an expression for a, as shown in Appendix B, is obtained:

$$a = \gamma\, m^{2/3} (l_0^3/m_0)^{2/3} \qquad 2.26$$

The shrinking core model can be expressed as:

$$\frac{dm}{dt} = -K\,\gamma\, m^{2/3} (l_0^3/m_0)^{2/3}\,\psi \qquad 2.27$$

with the boundary condition that $m = m_0$ and $\psi = \psi_0$ at $t = 0$

Now, defining M_0 and F_0 as the total initial number of moles of leachable zinc in all the particles in the leach and the total initial mass of all the particles respectively, and M and F as the corresponding values at any subsequent time t, it can be shown that:

$$-\frac{dM}{dt} = K\,\gamma\, F_0/(\rho l_0)(M/M_0)^{2/3}\,\psi \qquad 2.28$$

where ρ is the mass density. Refer to Appendix B for the derivation of this equation. If the particles are not all of the same size but have a size distribution of $f(l_0)$, then the total amount of leachable zinc remaining in the core is given by:

$$-\frac{dM}{dt} = K \int_{lmin}^{lmax} F_o \, \gamma \, (M/M_o)^{2/3} \, /(\rho l_o) \, \psi \, f(l_o) \, dl_o \qquad 2.29$$

where l_{min} and l_{max} are the minimum and maximum particle sizes. If the amount of leachable material is dependant on the particle size distribution, then:

$$\Sigma \frac{dM(l_{o_i})}{dt} = \frac{d}{dt} \Sigma M(l_{o_i}) \qquad 2.30$$

where $M(l_{o_i})$ represents the amount of leachable material in size class l_{o_i}. This represents i equations for i class fractions and are solved simultaneously.

2.1.3 Electrochemical shrinking core model

Combining equation 2.25 and equation 2.29, and rearranging, the equation describing the process is:

$$-\frac{dM}{dt} = K \int_{lmin}^{lmax} F_o \, \gamma \, (M/M_o)^{2/3} \, /(\rho l_o) \, \psi \, f(l_o) \, dl_o \qquad 2.31\,a$$

The solution conditions factor, ψ, can be represented in terms of the calculated redox potential, Eh, as follows:

$$\psi = \exp((1-\beta_1) \, Eh\mathcal{F}/RT) \qquad 2.31\,b$$

The solution redox potential depends on the total concentrations of the iron species and zinc species in solution and these are dependant on the extent of reaction. This means that Eh is a function of M only, that is, Eh = Eh(M). The electrochemical shrinking core model is a non-linear ordinary differential equation in one independent variable, t, the time since leaching commenced, and can only be solved by numerical techniques.

It is assumed that the other sulphide species, notably FeS, react at the same rate as the ZnS, but in proportion to the amount of non-zinc sulphidic material present (refer to Appendix B). It is also assumed that the ZnO layer that may be present around the particle reacts almost instantaneously with the acid in solution, and this is shown experimentally in Appendix H to be true. The extent of the ZnO layer may be determined by leaching the sphalerite in dilute sulphuric acid (0,05M H_2SO_4).

A modified Gear method for stiff differential equations was used from the I.M.S.L library to solve these differential equations (equations 2.30, which incorporates equation 2.31 for each particle size class), and no problems were experienced in the application of the package.

Equation 2.31 a and b represent the shrinking core behaviour of a set of particles of ZnS with a size distribution $f(l_s)$ dissolving by a mechanism of direct electrochemical oxidation. The assumptions made in the derivation of this model may be summarised as follows:

(i) Shrinking core behaviour;
(ii) Electrochemical dissolution by direct oxidative attack by ferric ion;
(iii) Kinetics given by Paul *et al* (1977) (equation 2.4);
(iv) Mineral surface potential is relatively large, or the concentration of Zn^{2+} is small, so that the first term of the denominator of equation 2.8 is negligible;

(v) $[S^-]$ intermediate is at steady state;

(vi) Electrochemical leaching occurs under conditions such that the sphalerite partial anodic current is negligible compared to that of ferrous ion oxidation on the mineral surface.

2.2 Oxidation of ferrous ion by dissolved oxygen.

The oxidation of ferrous ion involves two processes: (i) Mass-transfer of the oxygen gas to the liquid phase from the gaseous phase, that is, the dissolution of the oxygen, and (ii) the oxidation of the ferrous species by the dissolved molecular oxygen to the ferric state. Since the focus of this study is not on the mass-transfer characteristics, it is preferable to design the reaction conditions or apparatus such that the oxygen concentration reaches its saturated value very soon after the reaction begins, to ensure that gaseous-aqueous mass-transfer effects do not have a significant effect. This is achieved by increasing the stirrer speed sufficiently.

The results presented by Mathews and Robins (1972) and Chmielewski and Charewicz (1984) indicate that the oxidation of ferrous ion by dissolved oxygen has the form:

$$-\frac{d[Fe(III)]}{dt} = k_o\,[Fe(II)]^2[O_2]/[H^+]^b \exp(-E_a/RT) \qquad 2.32$$

where k_o is the overall reaction rate constant, E_a is the activation energy and b is a constant. Most authors agree that the reaction is second order in ferrous ion concentration and first order in oxygen concen-

tration, but disparity exists with regard to the dependance on hydrogen ion concentration.

The concentration of oxygen is dependant on the mass-transfer coefficient and the saturation concentration of oxygen in solution. The saturation concentration of oxygen is dependant on the partial pressure of oxygen gas, the temperature, and the concentration of dissolved electrolyte in the solution. As long as the concentration of dissolved gas is small and the temperature and pressure are far removed from the critical values for the gas, Henry's law is obeyed and the concentration of the gas, $[O_2]_{sat}$, in equilibrium with the partial pressure, $p(O_2)$, of the gas is given by

$$p(O_2) = [O_2]_{sat} H \qquad 2.33$$

where H is the Henry's law constant.

Since the oxygen reacts in solution, Henry's law does not apply to the total concentration of dissolved oxygen, but to the concentration of unreacted oxygen. In electrolyte solutions, the solubility of the oxygen is dependant on the concentration of electrolyte. Danckwerts (1970) described this 'salting out' effect in which the saturation concentration of oxygen decreases with increasing dissolved electrolyte by:

$$\log (S/S_o) = \Sigma\, h_i I_i \qquad 2.34$$

where S_o = solubility of oxygen in pure water
S = solubility of oxygen in an electrolyte solution
h_i = constant for a given ionic species i
I_i = ionic strength attributable to the ionic species i

Narita, Lawson and Han (1983) presented a modification of this result for oxygen which they found to be superior at higher electrolyte concentrations than that presented by Danckwerts (1970):

$$\log(S/S_s) = - \Sigma K_i C_i \qquad 2.35$$

where K_i = 'solubility constant' for all species i
C_i = molarity of species i

Values for K_i for different species i are presented in Appendix C.

The solubility of oxygen decreases with an increase in temperature for temperatures below 130° and a positive oxygen partial pressure, and is given by:

$$S_s = S_{298} \exp(1336/T - 4,48) \qquad 2.36$$

where S_{298} = solubility at 298°K, that is, $[O_2]_{sat}$ at 298 °K.

Combining equations 2.33, 2.35 and 2.36 to give the oxygen concentration:

$$[O_2] = p(O_2)/H_{298} \exp (1336/T - 4,48 - \Sigma K_i C_i) \qquad 2.37$$

Application of this equation involves the calculation of the concentrations of the various ionic species in solution, especially the concentrations of H^+, SO_4^{2-} and HSO_4^-. This calculation was performed by the subprogram EQUIL, the program that calculated the redox potential, as discussed in section 2.1.1. Thus the oxidation reaction is described by equation 2.32 and 2.37.

The assumptions made in the presentation of this model are:

(i) The overall kinetics of the ferrous ion oxidation reaction

are second order with respect to ferrous ion concentration, first order with respect to oxygen concentration, and proportion to the hydrogen ion concentration to some power.

(ii) The oxygen concentration is saturated at a level calculated by the correlation of Narita, Lawson and Han (1983) accounting for electrolyes in solution.

(iii) The hydrogen ion concentration is calculated by accounting for the complexes in solution (as discussed in section 2.1.1)

2.3 Leaching of sphalerite in the presence of oxygen.

A number of authors, including Jan, Hepworth and Fox (1976), Doyle, Masters, Webster, and Veltman (1976), and Forward and Warren (1960), suggested that the role of the oxygen in a solution of acidic ferric sulphate is to oxidise the ferrous species, rather than to contribute to the direct oxidation of the sphalerite. Mathews and Robins (1972) reported that zinc in solution does not catalyse the ferrous ion oxidation reaction. Thus, the leaching of the sphalerite mineral particles in the presence of dissolved oxygen and ferric ion can be modelled as the simultaneous solution of the leaching and the oxidation differential equations presented in sections 2.1 and 2.2, that is, equations 2.31 and 2.32. This assumes that the presence of sphalerite particles in solution does not catalyse or influence the ferrous ion oxidation reaction.

From the mathematical analysis developed above it is possible to test the propositions of this study. The proposition that the rate-limiting step of the dissolution of sphalerite is an electrochemical reaction can be verified by fitting the model derived in section 2.1 to the leaching data for sphalerite in the absence of oxygen. The proposition that the role of the oxygen in solution is primarily to oxidise ferrous ion in solution,

and therefore does not contribute directly to the dissolution is verified if the dissolution of sphalerite in the presence of oxygen is described by the simultaneous solution of the two differential equations describing each individual process.

These two rate equations, that is, equation 2.31 describing the leaching rate, and equation 2.32 describing the ferrous ion oxidation rate, are solved simultaneously using the modified Gear method for stiff differential equations, and this program is presented in Appendix K.

3. EXPERIMENTAL PROCEDURE AND RESULTS.

3.1 Experimental reagents and analysis.

3.1.1 Description of reagents.

The sphalerite obtained was a flotation concentrate from the Black Mountain ore deposit in the Cape. This material was chosen because of the possibility of it one day being commercially pressure leached in a process similar to that developed at MINTEK (Verbaan, 1981). The sample obtained was dried, and milled in a rod mill for five minutes per 500 grams to break agglomerates of smaller particles that had formed, and then tumbled for an hour to mix the whole sample. The particle size distribution for the milled sample was obtained from MINTEK by wet screening for size fractions above 38 micron and from a Warman cyclosizer on fractions below 38 micron. This distribution is presented in Table 3.1.

The chemical composition of each size fraction was obtained from MINTEK and is presented in Table 3.2. Mineralogically, the Black Mountain sphalerite is composed mainly of sphalerite (ZnS), with small amounts of galena (PbS), chalcopyrite ($CuFeS_2$), pyrrhotite ($Fe_{1-x}S$) and anglesite ($PbSO_4$).

Analytical grade sulphuric acid, ferrous sulphate crystals and ferric sulphate crystals were used. Distilled water was used to prepare all reagents to their desired concentration.

Table 3.1 Particle size distribution of Black Mountain sphalerite.

Fraction	Size (microns)	Mass % retained
0	212	0,00
1	150	0,74
2	106	4,26
3	75	8,02
4	53	12,74
5	38	11,44
6	29,81	5,31
7	23,58	10,28
8	16,57	10,78
9	11,75	8,13
10	8,35	5,84
11	-8,35	22,46 (by difference)

Table 3.2 Chemical composition of Black Mountain sphalerite.

Fraction	Zn	Fe	Cu	Pb	Mn	Si	S
1	48,5	9,15	0,54	2,57	1,73	1,96	29,1
2	49,4	9,62	0,66	0,97	2,00	1,32	30,9
3	49,5	10,3	0,63	0,80	2,11	1,26	31,4
4	49,5	10,6	0,52	0,70	2,12	1,30	32,0
5	48,8	10,9	0,41	0,63	2,04	1,14	31,2
6	48,6	11,7	0,34	1,33	1,66	0,65	31,3
7	51,1	9,95	0,32	1,15	1,75	0,89	30,6
8	51,4	9,98	0,29	1,31	1,59	0,81	30,8
9	52,5	8,80	0,28	1,36	1,42	0,67	31,6
10	53,5	8,46	0,27	1,36	1,29	0,53	31,8
11	41,9	9,09	0,63	9,37	1,20	1,23	27,9
Unscreened	49,7	10,09	0,54	2,95	1,80		27,5

3.1.2 Methods of chemical analysis.

The concentrations of zinc and iron in solution were measured on a Varian AA 1475 series atomic absorption spectrometer in the Department of Chemical Engineering at this university. The concentration of ferric ion was determined by titration with sodium thiosulphate, and the concentration of sulphuric acid was determined by titration with sodium carbonate. Refer to Appendix D for a description of these titration methods.

3.2 Apparatus.

Two sets of apparatus were used: a small 2 litre beaker in a constant temperature bath, and an 18 litre pressure reactor. The constant-temperature bath equipment was used when leaching in the absence of oxygen, while the pressure reactor was used for the oxidation of ferrous ion and leaching in the presence and absence of oxygen. The object of using the constant-temperature bath equipment was to study the initial rate of leaching more thoroughly. Diagrams of the equipment used are presented as figures 3.1 and 3.2.

3.2.1 Large pressure reactor.

The pressure reactor was a stainless steel, stirred vessel with a rounded bottom and a flat top. The top had three facility ports, a port for solids inlet, an inlet for gas supply, and an emergency outlet controlled by a bursting diaphragm. A pressure gauge and two vent taps were also attached to the lid. The reactor was heated by means of two electrical elements

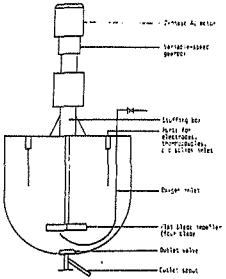

Figure 3.1 Diagram of large pressure reactor.

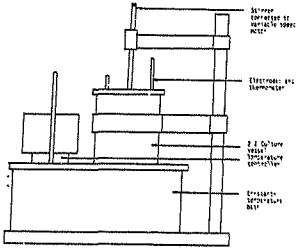

Figure 3.2 Diagram of constant-temperature bath equipment.

placed around the outside of the vessel, and the temperature was controlled by a proportional, integral and derivative controller. The reactor capacity was 18 litres. The gas supply, either nitrogen or oxygen, was controlled by a pressure regulator valve on the gas cylinder, and fed into the system by a stainless steel pipe and released through a single orifice to a point immediately below the impeller. The impeller was a four-blade, flat stainless steel impeller, driven by a variable speed motor. The speed was set using a stroboscope.

3.2.2 Constant-temperature bath equipment.

The constant-temperature bath equipment consisted of a 2,3 litre cylindrical glass culture-vessel fitted with a flat teflon lid to which two baffles had been attached. The lid had ports for a redox electrode, and for sample analysis. The lid was secured to the vessel with a flange. The contents of the vessel were stirred by a stainless steel impeller driven by a variable speed motor connected by a flexible cable drive. The speed was set using a stroboscope. The vessel was placed in the constant-temperature bath, which was controlled by a proportional controller. A Schott-Gerade Pt 62 combination electrode (reference: 3,5 M KCl S.C.E.) was immersed in the reacting solution and the redox potential measured on a Metrohm pH/mV meter.

3.3 Experimental procedures.

3.3.1 Procedure for leaching in the pressure reactor without oxygen present

A solution was made by dissolving ferrous sulphate and sulphuric acid in distilled water, and stored in a plastic drum. Ten litres of solution was tapped and reacted with hydrogen peroxide to produce the required amount of ferric ion, and poured into the reactor. The reactor was heated up under a pressure of nitrogen at approximately one atmosphere gauge to prevent any premature oxidation. The required amount of sphalerite was weighed to three figure accuracy, and once the temperature had stabilised, the sphalerite was added to the solution and the stop-watch started. The sphalerite was leached under a pressure of nitrogen. Approximately 15 ml samples were taken, filtered in a 200 ml membrane filter, and bottled. Dead volume in the sampling tube was removed immediately prior to taking the sample. Samples were analysed for ferric ion, total iron and zinc ion concentrations. After the run was completed, the solution was drained from the reactor, and the reactor was washed out with water or dilute sulphuric acid.

During the reaction the contents of the reactor were examined by lowering a torch bulb through one of the ports, and observing through another. This was to check that the sphalerite solids were thoroughly mixed, and did not float on the surface of the fluid. A vortex was observed in which the solids were well-mixed, contacting the leaching solution all the time.

3.2.2 Procedure for leaching in the constant-temperature bath reactor.

Sphalerite leaching without oxygen was also conducted in the constant-temperature bath equipment to examine the initial rate of leaching more thoroughly. A leaching solution was made up by dissolving solid ferric sulphate and sulphuric acid in distilled water and stored in a sealed glass container. Solution was then drawn from this supply so that a set of experiments would have the same initial concentration of ferric ion.

One litre of solution was taken from the make-up solution and poured into the leaching vessel in the constant-temperature bath. The bath was set at the required temperature and controlled to with 0,2 °K. The stirrer and the baffles were put in place, and the redox potential electrode was immersed to a sufficient depth in the solution. The required amount of ferrous sulphate, $FeSO_4.7H_2O$, was weighed to four figure accuracy and dissolved in the solution. The required amount of sphalerite was weighed to four figure accuracy. The temperature of the solution was allowed to rise, and once it had stabilised, the sphalerite was added to the solution and the stop-watch started.

Approximately 15 ml samples were extracted using a plastic syringe, fitted with some plastic tubing at regular intervals, and filtered in a 200 ml membrane filter. At the end of the leach, the solution was filtered and the solid residue collected. All containers were then washed in both acetone and distilled water for the next leach experiment.

3.3.3 Procedure for Fe(II) oxidation in the pressure reactor.

Ten litres of solution was made up by dissolving the required amount of ferrous sulphate and sulphuric acid in distilled water, and poured in the pressure reactor. The reactor was heated up under a pressure of nitrogen at approximately one atmosphere (gauge) to prevent any premature oxidation. Immediately prior to the beginning of the experiment, the nitrogen was vented. At the start, oxygen was fed through the system to remove any any remaining nitrogen, and then the pressure was allowed to build up to the required value. The stop-watch was started when the oxygen was first let into the pressure reactor. Approximately 15 ml samples were taken and analysed for ferric ion and total ion concentrations. Dead volume in the sampling tube was removed just prior to taking the s e. After the run was completed, the reactor was emptied and washed ou. th water or dilute sulphuric acid.

3.3.4 Procedure for leaching in the pressure reactor with oxygen present.

Solution was made up by dissolving the required amount of ferrous sulphate and sulphuric acid in distilled water, and then adding hydrogen peroxide to oxidise the required amount of ferrous sulphate to the ferric state. This solution was then poured into the pressure reactor, and heated up under a pressure of nitrogen. Just prior to the start, nitrogen was purged from the system. The sphalerite was poured into the reactor with distilled water in the form of a slurry, and any remaining solids were washed into the reactor with a small amount of distilled water. The stop-watch was started when the slurry was poured into the leaching solution. The reactor was then sealed, and the oxygen was turned on. Some oxygen was vented through the vent tap to remove any remaining nitrogen.

Approximately 15 ml samples were taken and filtered in a 200 ml membrane filter and bottled. Dead volume in the sampling tube was extracted just prior to taking the sample. Samples were analysed for ferric ion, sulphuric acid and total iron concentrations. At the end of the leach, the solution was filtered in a large five litre membrane filter, and the solid residue collected. The reactor was then rinsed and washed in distilled water.

3.4 Experimental results.

3.4.1 Results for sphalerite leaching without oxygen present.

The procedures outlined in section 3.3.1 were followed and the results are presented in Appendix E. All these experiments were conducted using Black Mountain sphalerite. Two g/l of unscreened sphalerite was leached in the pressure reactor. Solution containing ferrous ion only for these reaction experiments was taken from the same bulk solution so that they would have the same total iron concentration, and then oxidised to different extents using hydrogen peroxide. The results for three experiments at concentrations of 3,5 , 6,0 and 8,65 g/l ferric ion are shown in figure 3.3. All of these ferric ion concentrations are are in excess of the stoichiometric requirement for complete conversion. All three experiments show a sharp initial rate of dissolution dependant on the ferric ion concentration, but each rapidly slows off to reach a final conversion of zinc from the solid phase to the aqueous phase of about 40% after five hours at 80° C. This behaviour is irregular, since the conversion for run

39 at 3,5 g/l Fe(III) is higher than that for run 40 at 6,0 g/l Fe(III) after about 30 mins..

Run 28 on figure 3.3 is for a 20g/l sphalerite sample in 19,1 g/l Fe(III). Despite the increase in solids concentration, the final conversion remains at about the same level, that of 48%.

The reproducibility of the leach results was tested on a screened sample of sphalerite in the size range +74 -105 µm in the pressure reactor. Figure 3.4 indicates that these results are reproducible. A distinct decrease in the overall conversion between this and figure 3.3 is also evident.

The effect of agitation was tested on a sample in the size range +53 -74 µm in the pressure reactor. These experiments were conducted at the same initial conditions and are presented in figure 3.5. The rates of the first three runs, 56, 57, and 61 increase with stirrer speed; however, run 62 has the same initial rate as run 61 but the rate drops dramatically after that.

Figure 3.6 provides a comparison between five runs showing the effect of temperature, ferric ion concentration and stirrer speed. The ferric ion concentration of run 58 is double that of 57, and are both at 50°C, while run 59, at the same ferric ion concentration of run 58, is at 90°C. Comparison of runs 58 and 59 indicate that while there is a dramatic increase in the initial rate, the rates after about 15 minutes are comparable, indicative of chemical reaction control in the initial stages of reaction followed by diffusion control through a solid product layer, or product-layer passivation. Comparison of runs 62 and 63, at higher

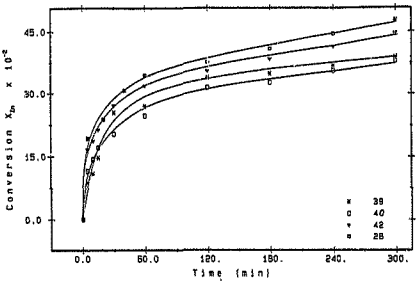

Figure 3.3 Leaching of sphalerite in an excess of ferric ions, indicating passivation of the reaction. Conditions: 80°C; unscreened ZnS; 8,95 g/l total iron; 450 RPM; 2g/l ZnS; 0,1M H_2SO_4, Run 39: 3,5 g/l; 40: 6,0 g/l; 42: 8,85 g/l Fe(III). Run 28: 19,1g/l Fe(III); 20g/l ZnS; 90°C

stirrer speeds than runs 57 to 59, confirm the result reported earlier that rate decreases dramatically at higher stirrer speeds.

The increase in temperature from 50°C to 90°C does increase the initial rate remarkably, again indicating chemical reaction or product-layer control at the beginning, followed by passivation.

Experiments in the constant-temperature bath equipment were undertaken to confirm that the leaching results presented above were not due to obvious experimental error, to measure the redox potential accurately, and to explore the initial rate more thoroughly. Runs F1, F4 and F5 were conducted at a constant ferric ion concentration varying the ferrous ion

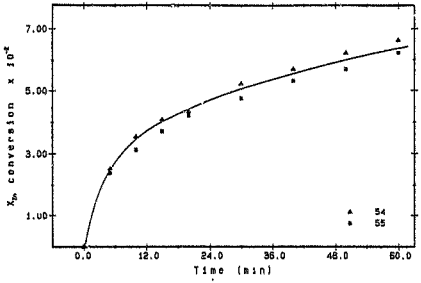

Figure 3.4 Reproducibility of leaching results. Conditions: 50°C; 210 RPM; 5,69 g/l Fe(III); 0.06 g/l Fe(II); 0,12 M H_2SO_4, 3 g/l ZnS; +74 -105 µm.

concentration. These results are presented in figure 3.7. A distinct decrease in rate is noted with the increase in ferrous ion, confirming the dependance of the initial rate on the concentration of the uncomplexed ferric ion in solution. Repeating these runs at a higher ferric ion concentration, F13, and a higher stirrer speed, F19, produced results that fell almost directly on one another, independent of the ferrous ion concentration, at *lower* conversions. This confirms the results obtained previously.

Data for the leaching of sphalerite from the Gamsberg ore deposit in acidic ferric sulphate media in the absence of oxygen is presented in the literature (Verbaan, 1980), and the analysis of this data in terms of the model derived in section 2.1.3, that is, equation 2.31, is presented in chapter 4.

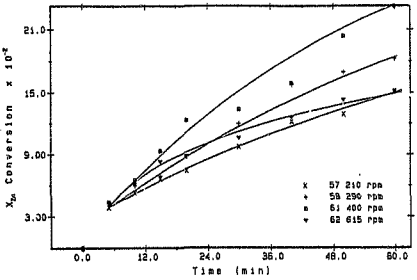

Figure 3.5 Effect of agitation. Conditions: 50°C; 5,69g/l Fe(III); 0,06g/l Fe(II); 0,12M H_2SO_4, 3g/l ZnS; +53 -74µm.

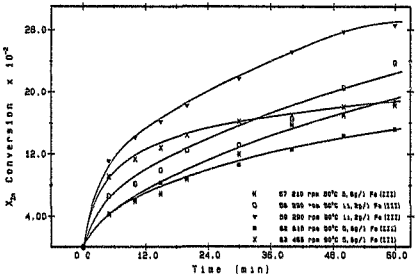

Figure 3.6 Effect of Fe(III) and temperature. Conditions: 0,06g/l Fe(II); 0,12MH_2SO_4, 3g/l ZnS; +53 -74µm.

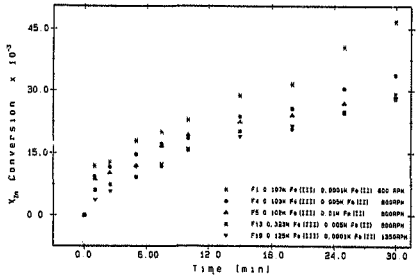

Figure 3.7 Typical results for the constant-temperature bath equipment. Conditions: 50°C; 3g/l ZnS; +74 -105µm; 0,12M H_2SO_4.

3.4.2 Experimental results for the oxidation of Fe(II) by oxygen.

Data obtained by the procedure outlined in section 3.3 2 are presented in Appendix F, and are discussed and analysed in chapter 5. Ferrous ion oxidation experiments were conducted under different conditions of Fe(II) concentration, temperature, oxygen partial pressure and acid concentration. The rate increases for an increase in Fe(II) concentration, temperature, and oxygen partial pressure, and decreases for an increase in the acid concentration. These results were found to be reproducible and typical results are presented in figure 3.8.

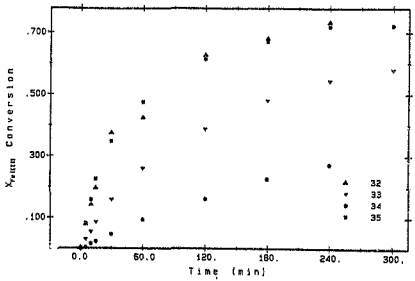

Figure 3.8 Fe(II) oxidation results. Conditions: 21,75 g/l total iron; 0,25M H_2SO_4, 450 RPM; Run 32: 353°K; 4,5 bar $p(O_2)$; 5,1 g/l Fe(III); 33: 343°K; 4,5 bar $p(O_2)$; 1,3 g/l Fe(III); 34: 333°K; 1,0 bar $p(O_2)$; 1,15 g/l Fe(III); 35: 353°K; 3,0 bar $p(O_2)$; 1,10 g/l Fe(III).

3.4.3 Experimental results for leaching with oxygen present.

The procedure for these experiments is outlined in section 3.3.3. The results from these experiments are presented in Figure 3.9 and 3.10, showing that the same problem experienced in the absence of oxygen occurs in the presence of oxygen as well. Figure 3.9 does indicate a slight increase in the final conversion for similar conditions as figure 3.3. Comparison of the results presented in figure 3.10 suggest that the addition of oxygen to the system results in significantly increased initial rates, followed by the same decrease in rate at the end of the leach. The difference between runs 63 and 64 shows clearly that the addition of oxygen has a marked effect.

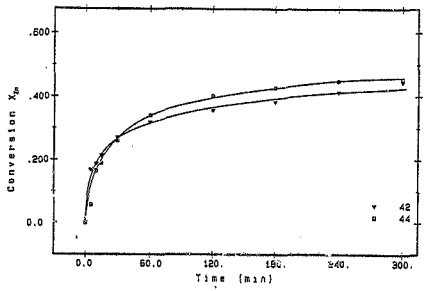

Figure 3.9 Leaching of sphalerite in the presence of oxygen.
Conditions: 80°C; 7,35 g/l Fe(III); 8,85 g/l total iron; 2g/l ZnS; 0,12M H_2SO_4.
Run 42: no oxygen; 44: 0,5 bar $p(O_2)$.

Data for the leaching of a sphalerite from the Gamsberg ore deposit in acidic ferri sulphate media in the presence of oxygen is presented in the literature (Verbaan, 1981), and analysis of this data in terms of the model presented in chapter 2, that is, the simultaneous numerical solution of equations 2.31 and 2.32, is presented in chapter 6.

The leaching results for Black Mountain sphalerite are discussed in section 4.1, and the results for the leaching of Gamsberg sphalerite are analysed in section 4.2. The theoretical analysis presented in section 2.2 is applied in chapter 5 to the experimental results for the ferrous ion oxidation reaction presented in this chapter. Results for the leaching

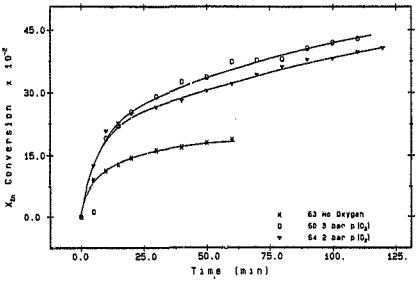

Figure 3.10 Leaching of sphalerite in the presence of oxygen.
Conditions: 90°C; 465 RPM; 0,0602g/l Fe(II);
0,12M H_2SO_4, +53 -74 µm;
60: 11,5g/l Fe(III); 9g/l ZnS; 3 bar $p(O_2)$.
64: 5,35g/l Fe(III); 16g/l ZnS; 2 bar $p(O_2)$.
63: 5,6 g/l Fe(III); 3 g/l ZnS; no oxygen.

of Black Mountain sphalerite and Gamsberg sphalerite in the presence of oxygen are analysed in chapter 6.

4. ANALYSIS OF EXPERIMENTAL LEACHING RUNS IN THE ABSENCE OF OXYGEN.

4.1 Leaching of Black Mountain sphalerite without oxygen.

4.1.1 Leaching results for conditions of an excess ferric ion.

The leaching of Black Mountain sphalerite in a solution containing an excess of ferric ion show a sharp initial rate of dissolution dependant on the ferric ion concentration, but in each the rate dramatically drops to a final conversion of about 40 - 50%. These results are reported in section 3.4.1 and plotted as figure 3.1.

The low final conversion could be attributed to a number of causes:

(i) Experimental error.

Sphalerite tends to adhere to solid surfaces, and the full sample may not contact the solution, or, because the material is finely divided, the reactor may act as a flotation cell with all the material floating on the surface of the solution. Examination of the conditions within the reactor with a torch bulb indicated that since there were no baffles in the reactor, the solution was stirred in a vortex in which the solids would recirculate back into solution. Examination of the reactor after the experiment indicated a significant amount of material did not remain on the walls or on the probes, and a mass balance for zinc confirmed this.

(ii) Non-oxidative inhibition.

The production of H_2S could inhibit the reaction as demonstrated by Pawlek (1969), who completely stopped the reaction by applying a partial pressure of 2 atm H_2S. Hydrogen sulphide was smelled at the beginning of the reaction; since this can be detected at concentrations of parts per billion and higher concentrations would have caused irritation, this could not have inhibited the reaction.

(iii) Passivation due to formation of an impervious product layer.

The production of lead sulphate, which is insoluble, could form a passive layer around the particle, or the the sulphur may form an impervious layer through which the passage of ferric ion is inhibited. Samples of these residues were sent to the Mineralogical Division of MINTEK for analysis for a $PbSO_4$ layer or for layers of sulphur that may inhibit the reaction. These mineralogical test results are discussed in section 4.3.

A 200g sample of sphalerite was leached to a conversion of 0,33 (calculated from the zinc concentration in solution) and the final residue was sent for analysis. These results are presented in table 4.1. The mass % for these elements, based on the concentration conversion for zinc and the residue results for Mn, Fe, are also presented. This represents a component balance for zinc and sulphur. There is a good comparison between these results, confirming that the sulphur reports as elemental sulphur, forming an extensive product layer around the particle. This may result in product-layer diffusion control.

According to Levenspiel (1972), the shrinking core model with diffusion through the product layer as the controlling mechanism can be expressed in terms of the conversion, X, as:

Table 4.1 Analysis of sphalerite leach residue.			
Element	Mass % measured[1]	Mass % calculated[2]	Mass % unleached[3]
Zn	42,4	41,4	49,7
S^0	10,1	10,02	-
S^{2-}	25,1	20,3	27,5
Mn	1,43	1,42	1,80
Fe	8,84	8,80	10,09

[1] In residue.

[2] Based on solution analyses.

[3] Data from table 3.2.

$$1 - 2/3X - (1 - X)^{2/3} = kt \qquad 4.1$$

where $X = 1 - M/M_0$

k = a rate constant;

for spherical particles. Figure 4.1, a plot of the left-hand side of equation 4.1 against time, illustrates that the controlling mechanism might be diffusion through the product layer in the first 30 minutes, but this rapidly deviates from the predicted straight-line behaviour. The initial rate of leaching was studied more closely in the constant-temperature bath equipment and the results from this examination are analysed in section 4.1.4.

A mechanism other than product-layer diffusion, such as the formation of a coat that completely protects the particle core from the oxidant is dominant in this case.

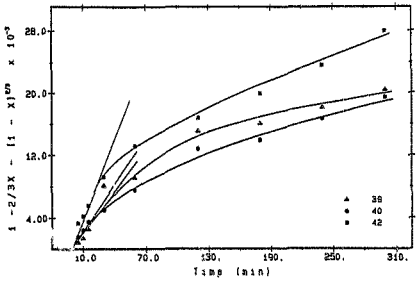

Figure 4.1 Diffusion through product layer plot for runs 39, 40, and 42.
Conditions: 80°C; unscreened ZnS; 8,95 g/l total iron;
450 RPM; 2g/l ZnS; 0,1M H_2SO_4.
Run 39: 3,5 g/l; 40: 6,0 g/l; 42: 8,85 g/l Fe(III).

4.1.2 Effect of agitation.

The effect of agitation on the leaching rate of Black Mountain sphalerite was tested and the results are reported in section 3.4.1, and plotted as figure 3.3. These results show an increase in rate for an increase in stirrer speed for three runs at 210, 290 and 400 RPM. For another run at 615 RPM the initial rate was the same as that at 400 RPM, but the rate dropped dramatically after that, clearly indicating that passivation is enhanced by higher agitation. Jan *et al* (1976) attributed the dependency of the rate on agitation to the oxidation of H_2S formed at the surface of the particle by ferric ion (refer to equation 1.10). It is conceivable that at lower stirrer speeds a non-oxidative dissolution occurs, while at higher stirrer speeds a direct oxidation mechanism forms a different type of sulphur, which passivates the material. This is a more difficult

proposition to test using this experimental design since the overall products of both reaction mechanisms are the same. Neither Scott and Nicol (1978) nor Verbaan (1977, 1980) noted any dependance on agitation, and this was as surprising a result as the inhibition of the reaction itself.

4.1.3 Effect of temperature.

The effect of temperature was tested, and the results are reported in section 3.4.1, and plotted as figure 3.4. Comparison of two sets, one at a higher ferric ion concentration and lower stirrer speed (runs 58 and 59), and the other at a lower ferric ion concentration and higher stirrer speed (runs 62 and 63), indicate that while there is an increase in initial rate for an increase in temperature, the rates after about 15 mins. are comparable. This is indicative of chemical reaction or diffusion through a product layer control in the initial stages of reaction. The results at higher stirrer speeds confirm the result reported in section 4.1.2 that passivation is enhanced at higher stirrer speeds. It is difficult to make any conclusions as to the nature of this passivation mechanism from these results.

4.1.4 Analysis of the initial rates of leaching.

Leaching experiments in the constant-temperature bath equipment were undertaken in order to examine the initial rates and to monitor the redox potential. These results are presented in section 3.4.1. A plot fitting the left hand side of equation 4.1 against time for this data is presented as figure 4.2. A straight line is observed, indicative of diffusion through the product layer being the rate controlling step in the initial

stages of reaction. The slope is dependant on the ferrous ion concentration for constant ferric ion concentrations, and therefore the initial rate is dependant on the diffusion of uncomplexed ferric ions through the sulphur layer. However, increasing the ferric ion concentration or the stirrer speed results in lower conversions. This defies an explanation in terms of sphalerite reactior kinetics proposed in this study or in the literature, and again points to the formation of an impervious product layer on the surface of the particle. The observed dependance of the initial rate on diffusion through a product layer is probably due to the formation of an impervious product layer on the surface resulting in passivation.

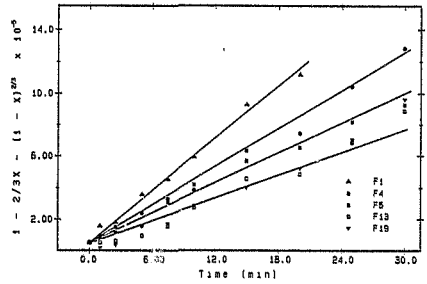

Figure 4.2 Diffusion through product layer plot, indicating the effect of an increase in Fe(III), Fe(II), and agitation.
Conditions: 50°C; 3g/l ZnS; +74 -105 µm; 0,12M H_2SO_4.
F1 0,107M Fe(III), 0,0001M Fe(II), 800 RPM;
F4 0,103M Fe(III), 0,003M Fe(II), 800 RPM;
F5 0,102M Fe(III), 0,010M Fe(II), 800 RPM;
F13 0,323M Fe(III), 0,005M Fe(II), 800 RPM;
F19 0,125M Fe(III), 0,0005M Fe(II), 1350 RPM;

Monitoring the redox potential did not illuminate the problem, since it followed the extent of reaction very closely. The kinetics proposed for this reaction in chapter 2 cannot be verified by monitoring the redox potential during a batch leach, since the redox potential represents both the driving force for reaction, and the extent of reaction.

4.2 Analysis of leaching data for Gamsberg sphalerite.

Verbaan (1980) leached a natural sphalerite concentrate from the Gamsberg deposit in the Cape and reported data that the model derived in chapter 2 can be fitted to.

The parameters for the model presented in section 2.1.3, that is, equation 2.31, incorporating the prediction of the redox potential by subprogram EQUIL, are estimated by an ordinary least squares criterion, in which the sum of squared differences between the measured concentration data and the model prediction are minimised. Since this model has only two parameters:

K, the rate constant (mol/m^2min);

and

$k' = (1-\beta_i)\mathcal{F}/RT$, the symmetry constant (V^{-1});

a diagram of the sum of squared differences surface can be drawn as a contour plot to illustrate the minimum. Figure 4.3 illustrates this surface for data measured by Verbaan (1980) for his data sets four to nine. The islands present along the minimum are due to interpolation error from

the contour plotting routine, and should rather be joined together as a closed banana shape.

This diagram illustrates a valley of almost equal depth in the sum of squares surface, and a choice of any set of parameters along the bottom of the valley will yield a fit that is almost as good as any other. However, there is a shallow minimum which has been obtained by using a golden section search on the parameter K at various constant values of k^1. These results are presented in Appendix I.

This banana shape and the distinct minimum indicate a slight linear dependence of the sensitivity coefficients, which are the partial derivatives of the model equation with respect to the model parameters (Beck and Arnold, 1977). If the sensitivity coefficients were linearly dependant, the valley would be equally deep, and there would be no unique minimum. This indicates either the model is not very good at describing the experimental data, or the data has not been selected over a wide enough range, in much the same way as a poor estimate of the activation energy will be obtained from rate data if the temperature range is too small. The more likely event for this model is that the range of initial redox potentials is not large enough, although this is not necessarily the case. The measured redox potential ranged between 420 mV and 540 mV Ag/AgCl. If this model is to be tested thoroughly, the experiments must be conducted over a greater range of redox potentials.

The confidance region is obtained from the likelihood ratio, given by Beck an Arnold (1977) as:

$$(Ss - Rr)(n - p)/(Rrp) = F_{1-\alpha}(p,n-p) \qquad 4.2$$

where p = number of parameters;

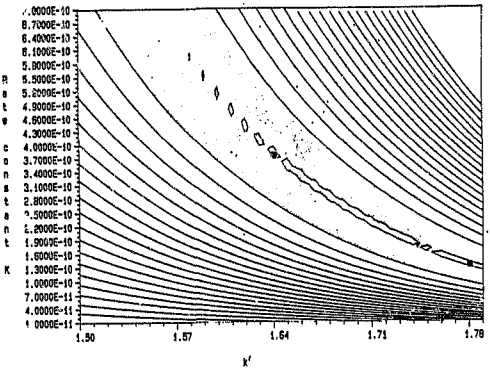

Figure 4.3 Sum of squared differences surface for Gamsberg leaching results without oxygen indicating the valley in the surface. The minimum occurs along the shaded ridge. The first contour is at a sum of squares value of $1{,}15 \times 10^{-6}$ and the levels rise in step of $1{,}5 \times 10^{-5}$ above that.

n = number of data points;
Rr = minimum sum of squares;
Ss = 1-α confidence contour level;
F = F distribution.

From this the 95% confidence contour level is calculated as the $1{,}556 \times 10^{-5}$ level. This corresponds closely to the second level on figure

4.3, that is the $1{,}615 \times 10^{-5}$ level. The 95% confidence region is shaded in on figure 4.7. The values of the parameters at the best fit are:

$K = 0{,}1956 \times 10^{-9}$ mol/m^{2}min;
$k' = 17{,}3\ V^{-1}$.

The parameter fit is displayed in figure 4.4. The points represent the measured data and the lines calculated by the model using the best-fit parameters. The conversion at time t=0 represents the amount of zinc oxide layer leached before sphalerite leaching occurs. This diagram illustrates that the model, despite the problems mentioned above, does fit the experimental results well. Figure 4.5 represents a log-log plot of the measured initial rate of reaction against the measured redox potential, indicating that this model is empirically sound. The slope of the straight line has a value of $15{,}6\ V^{-1}$ which corresponds well to the best-fit value of k' of $17{,}3\ V^{-1}$.

The value of β_i in the parameter k' was assumed to be constant with temperature, and thus the value of k' at temperatures other than 65°C was calculated. Using values of k' calculated in this way, the parameter K was fitted using a golden section search for data sets 24, 25 and 26 of Verbaan's work at 25, 45 and 85°C respectively. These results are presented in Appendix I. Plotting the Arrhenius diagram for these rate constants, an activation energy of 79,4 kJ/mol was obtained

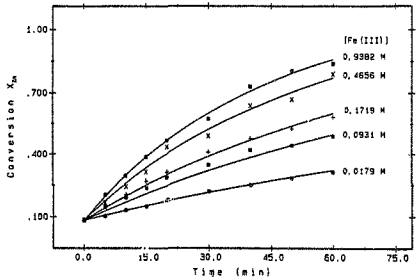

Figure 4.4 Equation 2.31 fitted to Gamsberg leaching data for parameters at the minimum sum of squares for increasing ferric ion concentrations. Conditions are 65°C; 0,1M sulphuric acid; 0,038M Fe(II). The initial conversion is due to the ZnO layer.

Therefore the leaching of Gamsberg sphalerite is well-described by the following expression:

$$-\frac{dM}{dt} = 390{,}3\exp(-79{,}4/RT)\ A_s\ (M/M_s)^{2/3}\exp(0{,}504\bar{F}h/RT) \qquad 4.3$$

where $A_s = \int F_s\ Y\ f(l_s)/(pl_s)\ dl_s$

A_s was measured by Verbaan (1980) using a BET surface area technique and had a value of 7,355 m^2 for a 5g sphalerite sample leached.

4.3 Results from the mineralogical study, and discussion.

The main difference between the sphalerite from Black Mountain and that from Gamsberg, which leached to almost 10% conversion of zinc, is the amount of lead. The Gamsberg deposit assays 7,4% Zn and 0,5% Pb, while the corresponding values for the Black Mountain deposit are 2,2% Zn and 3,0 - 4,5% Pb (Hammerbeck and Mehliss, 1976). Examination of the chemical compositions of the concentrates, given in section 3.1." and by Verbaan (1980), indicate that this is the case. The Gamsberg concentrate assays 0,47% Pb, while the Black Mountain concentrate assays 2,95% Pb.

This suggests that the mechanism for passivation could be the formation of an insoluble coat of $PbSO_4$ on the surface of the particle which would prevent any further reaction. Samples of leach residues from runs 39 and 42, together with an unleached sample, were submitted for mineralogical

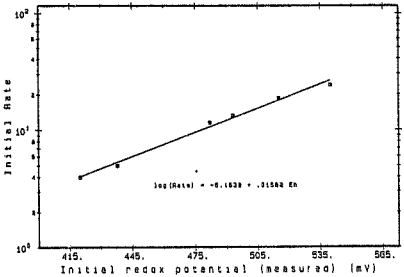

Figure 4.5 Initial rate of leaching against the measured redox potential for Gamsberg sphalerite. Data taken from Verbaan (1980).

analysis. These results indicated that while $PbSO_4$ does form, it is contained to the regions above the PbS deposits. This is clearly illustrated in figure 4.6.

The formation of an impervious sulphur layer could inhibit the reaction. Nattrass (1985), in a personal communication, described a similar problem in which about 40% of the zinc from Black Mountain material remained unleached. The residue was then treated in a Soxhlet epparatus with perchloroethylene to remove the sulphur layer, and subsequent leaching was still inhibited. On mineralogical investigation, elemental sulphur was still found on this material. He proposed that trace heavy metals could contaminate the sulphur layer, lower the melting point, and thereby act as a passivation mechanism.



Figure 4.6 The formation of $PbSO_4$ above the galena deposit. Back-scatter electron image showing the occurrence of anglesite (1) related to a galena intrusion (2) in sphalerite.

Kuzminkh and Yakoutova (1950) leached two mineralogically different natural sphalerites. They reported that the sphalerites leached at similar initial rates under equivalent conditions. However, for similar conditions, an excess of 80% conversion was achieved for the one, while only 33% was obtained for the other. They proposed that the fine intergrowth of different minerals was such that the ZnS was combined in a solid solution as a complex $ZnFeS_2$ compound, which would be stable in acidic ferric sulphate media.

Other metal sulphides are known to passivate. Wadworth (1972) reported that covellite (CuS) reacted rapidly initially, but soon decreased. He attributed this to the build-up of elemental sulphur. In the discussion of the kinetics of chalcopyrite ($CuFeS_2$) dissolution, he stated that the parabolic kinetics suggested diffusion through the product layers as the controlling mechanism. If the reaction was electrochemical, this would mean that the pores would have to be small. He also suggested that dehydration of the diffusion ions, or flow of polymeric sulphur units might be involved. Parker, Paul and Power (1981) observed that a surface film forms on chalcopyrite, and slows the transport of ions. They proposed that this film is a metal-deficient polysulphide, such as $CuFeS_4$.

The X-ray analysis indicated that the distribution of Fe and Zn in the sphalerite grains was normal, and that a substantial layer of sulphur coated the particle. However, it is difficult to determine whether any of the above-mentioned causes could be occurring. To continue any analysis and work in this area is beyond the scope of this work.

The initial rates are increased by increase in ferric ion concentration (figure 4.1), agitation (figure 4.3), temperature (figure 4.4), and oxy-

gen concentration (figure 4.7). These results are all compatible with the results obtained and the kinetics proposed by Jan *et al* (1976). However, an increase in ferric ion concentration and agitation (figure 4.4 and 4.5) beyond a certain level resulted in enhanced passivation. The mechanism of this passivation is not known, but is probably related to the formation of a metal polysulphide, or contamination of the elemental sulphur layer such that it forms a molten coat around the particle.

In conclusion, although the Black Mountain sphalerite leaching mechanism may incorporate an electrochemical step, it appears that the passivation mechanism controls the rate. On the other hand, under the conditions tested, the Gamsberg sphalerite leaching appears to be electrochemically rate controlled.

In chapter 5 the results for the ferrous ion oxidation reaction are analysed.

5. ANALYSIS OF EXPERIMENTAL Fe(II) OXIDATION RESULTS.

5.1 Determination of the second order rate constant.

Based on the literature reviewed in section 1.1.2 and the model presented in section 2.2, the ferrous ion oxidation reaction was assumed to be second order in ferrous ion concentration and first order in oxygen concentration. This is expressed by the rate equation:

$$\frac{d[Fe(III)]}{dt} = - k [Fe(II)]^2 \qquad 5.1$$

where $k = k_o [O_2]/[H^+]^b \exp(-E_a/RT)$

Integration of this for constant $[O_2]$, $[H^+]$ and temperature, w.r.t. time, t, gives:

$$1/[Fe(II)] = kt + 1/[Fe(II)]_o \qquad 5.2$$

where $[Fe(II)]_o$ = Fe(II) concentration at time t = 0.

The second order rate curve, that is, a plot of 1/[Fe(II)] against time, will be a straight line if this is a second order reaction, and will be curved in the initial stages of the reaction if there are any mass-transfer effects. The value of k is determined from the slope of this line in the region in which the reaction is proposed to be second order.

Both Iwai *et al* (1982) and Chmielewski and Charewicz (1984) presented second order plots that deviated from the expected straight line in the latter stages of the reaction (refer to section 1.1.2). Typical results obtained are illustrated in figure 5.1, and from the initial straight line curves it is concluded that mass-transfer is not important at a stirrer speed of 450 rpm, and that similar deviations to those reported by Iwai *et al* (1982) and Chmielewski and Charewicz (1984) are also present. The values of k were obtained from the initial slopes for all the oxidation runs presented in Appendix F and are presented in Appendix J.

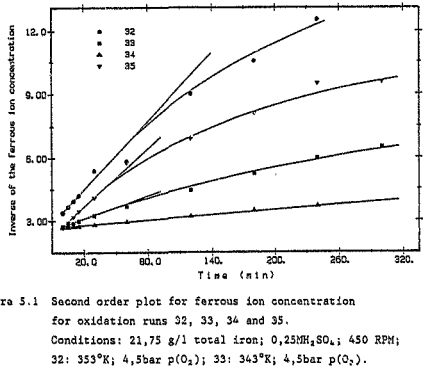

Figura 5.1 Second order plot for ferrous ion concentration for oxidation runs 32, 33, 34 and 35. Conditions: 21,75 g/l total iron; 0,25M H_2SO_4; 450 RPM; 32: 353°K; 4,5bar $p(O_2)$; 33: 343°K; 4,5bar $p(O_2)$. 34: 333°K; 1,0bar $p(O_2)$; 35: 353°K; 3,0bar $p(O_2)$.

5.2 Dependance of Fe(II) oxidation rate on hydrogen ion concentration.

The concentration of the hydrogen ion, for the determination of the dependance of the rate on the hydrogen ion, was also calculated by the subprogram EQUIL, and the concentration of oxygen in solution was calculated from the semi-empirical equation presented by Narita, Lawson and Han (1983). The use of this correlation is discussed in section 2.2. A plot of the apparent rate constant, $k/[O_2]$, for the oxidation rate data presented in Appendix J against the calculated hydrogen ion concentration, $[H^+]$ on log-log axes is a straight line with slope b. This plot is presented as figure 5.2, from which it can been seen that the rate is inversely proportional to the hydrogen ion concentration to the power 0,36. Keanan (1969) reported a similar value, that of 0,35, while Mathews and Robins (1972) reported a value of 0,25. This deviation can be attributed to the way in which the hydrogen ion concentration is calculated. Mathews and Robins (1972) measured the pH of their sample at ambient temperature, and calculated the hydrogen ion concentration from this. Therefore, this result is in agreement with previous research, and a value of 0,35 was used in subsequent calculations.

5.3 Dependance of Fe(II) oxidation rate on temperature.

An Arrhenius plot, that of $\log(k[H^+]/[O_2])$ against 1/temperature has a slope of E_a/R and an intercept of $\log(k_o)$. The Arrhenius plot for the ferrous ion oxidation reaction is illustrated in figure 5.3.

From the slope of the Arrhenius diagram, the activation energy, E_a, is 68,6 kJ/mol and the rate constant, k_o, is $1,248 \times 10^{11}$. Table 5.1 com-

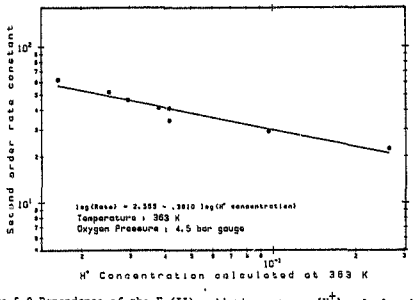

Figure 5.2 Dependance of the Fe(II) oxidation rate on $[H^+]$ calculated by subprogram EQUIL, representing oxidation runs 2-27 in table J.2.

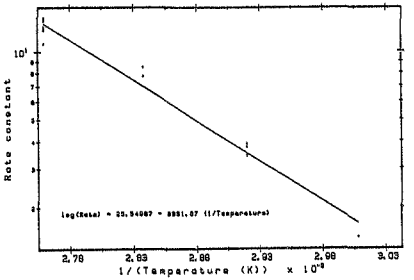

Figure 5.3 Arrhenius plot for Fe(II) oxidation, for all oxidation runs.

pares the results obtained in this study with those reported in the literature.

Therefore, the initial rate of oxidation is described by:

$$\frac{d[Fe(II)]}{dt} = 1,248x10^{11}[Fe(II)]^2[O_2]/[H^+]^{0,35}\exp(-68,6/RT) \quad 5.3$$

If this reaction is to be more thoroughly understood, a more detailed analysis is required, probably studying the formation of iron complexes in solution, and the effect these complexes have on the oxidation reaction.

Table 5.1 Comparison of ferrous ion oxidation kinetic expressions.

Authors	Kinetic equation for d[Fe(III)]/dt	E_a kJ/mol
Huffman & Davidson (1956)	$k_s[Fe(II)]p(O_2) + k_t[Fe(II)]^2p(O_2)$	67,9
Keenan (1969)	$k[Fe^{2+}]^2[O_2]^{1,04}[H^+]^{-0,35}$	94,1
Mathews & Robins (1972)	$k[Fe^{2+}]^{1,84}[O_2]^{1,01}[H^+]^{-0,25}$	73,7
Chmielewski & Charewicz (1984)	$k[Fe(II)]^2p(O_2)$	56,9
Iwai, Majima & Awakwa (1982)	$k[Fe^{2+}]^2[O_2] + [SO_4^{2-}][Fe^{2+}]^2p(O_2)$	51.6
This study	$k[Fe(II)]^2[O_2][H^+]^{-0,36}$	68,6

6. ANALYSIS OF EXPERIMENTAL LEACHING RUNS IN THE PRESENCE OF OXYGEN.

6.1 Analysis of leaching of Black Mountain sphalerite with oxygen present.

The results for the leaching of Black Mountain sphalerite in acidic ferric sulphate media with oxygen present are presented in section 3.4.3. These results indicate that the addition of oxygen to the sphalerite leaching system results in higher initial rates, followed by the same final rate and passivation behaviour.

It is concluded that the passivation behaviour observed for Black Mountain sphalerite in acidic ferric sulphate solutions in the absence of oxygen, and discussed in chapter 4, also occurs when oxygen is added to the system.

6.2 Prediction of Gamsberg leaching data with oxygen present.

The parameters obtained in sections 4.2 and 5.3, that is, equations 4.3 and 5.3, were used directly to predict the data presented by Verbaan (1981) for sphalerite leached in the presence of oxygen and ferric ion. These results are presented in figures 6.1 and 6.2. This sphalerite was the same Gamsberg material reported in Verbaan's (1980) earlier paper, the leach parameters of which have been fitted in section 4.2. Figure 6.1 shows the curve for the extraction of zinc as the reaction proceeds with time, and figure 6.2 shows the way in which the ferrous and ferric

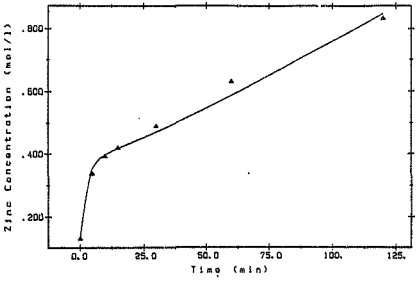

Figure 6.1 Prediction of the leaching of Gamsberg sphalerite in the presence of oxygen: zinc extraction. Conditions: 90°C 116 kPa $p(O_2)$, 35 g/l Fe(III), 200 g/l ZnS. Points are measured and lines are predicted.

reaction. The points are the measured data, and the lines and the predicted curves. The extraction of zinc indicated a good fit over the entire curve, while figure 5.4 show a deviation at about 60 mins.. However, for a predicted curve in which the ferric ion concentration changes dramatically and hence the driving force, the redox potential, this is a satisfactory result, confirming the electrochemical proposition. Lack of such data prevents any meaningful interpretation to be made about the observed deviation at 60 mins..

The dissolution of Gamsberg sphalerite is well described by the electrochemical shrinking core model developed in chapter 2 and the overall oxidation of ferrous ion by oxygen in the 0 - 11 g/l Fe(III) concentration range is well described by the propositions made in chapter 2, and conforms well with the results reported previously (table 5.1).

The simultaneous solution of rate equations 4.3 and 5.3 describes the leaching of Gamsberg sphalerite in the presence of oxygen satisfactorily (figures 6.1 and 6.2). From this it is inferred that the dissolution of Gamsberg sphalerite is controlled by an electrochemical reaction at the particle surface.

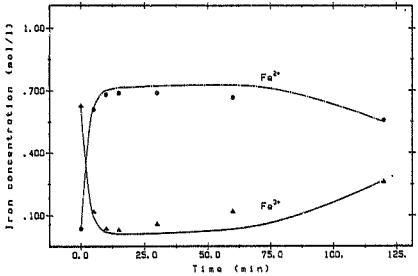

Figure 6.2 Prediction of the leaching of Gamsberg sphalerite in the presence of oxygen: changes in the iron concentrations, for the same run as figure 6.1.
Conditions: 90°C, 116 kPa $p(O_2)$, 35 g/l Fe(III), 200 g/l ZnS. Points are measured and lines are predicted.

7. CONCLUSIONS AND RECOMMENDATIONS.

A review of the literature suggested that the kinetics of the dissolution of sphalerite are dependant on the type of sphalerite being leached. Every general category of rate-controlling mechanism has been proposed. Even though the reaction at the surface is thought to be electrochemical in nature, a model incorporating this proposition as the rate-controlling step has not been proposed for the leaching of sphalerite. Much of the research reported has been of a qualitative nature, with perhaps two oxidants, oxygen and ferric ion, present in solution. A review of the literature for ferrous sulphate oxidation by dissolved oxygen indicated that the reaction occurs in a complex fashion, with the consequence that several kinetic expressions have been proposed. General agreement is that the reaction was second order in ferrous ion concentration, at least at low conversions to ferric ion, and first order in oxygen concentration. The role of the hydrogen ion is a disputed point. (Refer to chapter 1).

Experimental work was undertaken using a natural sphalerite from the Black Mountain ore deposit to (i) test the electrochemical proposition for the dissolution of sphalerite in the absence of oxygen, (ii) obtain a reliable expression for the ferrous ion oxidation reaction, and (iii) test the proposition that leaching in the presence of oxygen is described by the simultaneous solution of both kinetic expressions found in (i) and (ii). These propositions were also tested using data from the literature. (Refer to chapters 2 and 3).

The Black Mountain sphalerite was leached under different conditions of ferric ion concentration, agitation, temperature, and oxygen partial pressure. Passivation occurred in all samples, resulting in an maximum conversion of about 40% for zinc. This passivation is not caused by the formation of an insoluble $PbSO_4$ layer on the particle, but is probably

related to the formation of a $ZnFeS_2$ complex, or a similar polysulphide, such as $ZnFeS_4$, which is stable in acidic ferric sulphate media. A more thorough investigation of this phenomena is required. (Refer to section 4.3). Because of the passivation behaviour exhibited by Black Mountain sphalerite, no attempt was made to fit a modal to the leaching data.

The leaching of sphalerite from the Gamsberg ore deposit in the absence of oxygen is reported in the literature, and this data is well described by the electrochemical model developed in chapter 2. The kinetics of this dissolution are therefore controlled by an electrochemical reaction occurring at the surface of the particle. (Refer to section 4.2).

The oxidation of ferrous sulphate by dissolved oxygen was examined, and is well described in the initial stages of reaction, that is, in the 0 - 11 g/l ferric ion concentration range, by second order kinetics with respect to ferrous ion concentration, and first order kinetics with respect to oxygen concentration. The dependance of the rate on the hydrogen ion concentration is proportional to the power -0,36, and the activation energy is 68,6 kJ/mol. This is in good agreement with several authors (refer to table 5.1). A more thorough investigation of this reaction is required in the higher ferric ion concentration region where the rate deviates from second order kinetics with respect to ferrous ion concentration.

The leaching of the same Gamsberg material in the presence of oxygen and ferrous sulphate is well described by the simultaneous solution of the differential equations describing the individual processes, indicating that the ferric ion is responsible for leaching, and the oxygen is responsible for the regeneration of the ferric ion. (refer to section 6.2).

The differences between the leaching characteristics of the two different sphalerites emphasises again how importan. the mineralogical factors, such as grain size, lead content, and other trace metals and minorals, are. An investigation of the effects of these types of factors is recommended.

8. REFERENCES.

Beck, J. and Arnold, R. (1977) '*Parameter estimation in engineering and science*', John Wiley and Sons, New York.

Bockris, J. and Reddy, A.K.N. (1970) *Modern Electrochemistry*', vol. 2, John Wiley and Sons, New York.

Chmielewski, T., and Charewicz, W.A. (1984) '*The oxidation of Fe(II) in aqueous sulphuric acid under oxygen pressure*', Hydromet., vol. 12, pp. 21-30.

Danckwerts, P.V. (1970) '*Gas-liquid reactions*', McGraw-Hill Book Co., New York.

Doyle,D.N., Masters,I.M., Webster,I.C., and Veltman,H. (1978) '*Acid pressure leaching of zinc concentrates with elemental sulphur as a by-product*',Eleventh Commonwealth Mining and Metallurgical Congress, Hong Kong, 1978. Jones,M.J., (ed), Institute of Mining and Metallurgy, London pp. 645-653.

Dry, M.J. (1984) '*Kinetics of leaching a low grade matte in ferric sulphate solution*', Ph.D. Thesis, University of the Witwatersrand, Johannesburg.

Dutrizac,J.E. and MacDonald,R.J.C., (1974) "*Ferric ion as a leaching medium*', Minerals Sci. Engng., vol.6, no.2, pp 59-100

Forward,F.A., and Warren,I.H. (1960) '*Extraction of metals from sulphide ores by wet methods*', Met. Reviews, vol.5, no.18, pp. 137-164.

Hammerback, E.C.I., and Mohliss, A.T.M. (1976) '*Zinc*", in

Mineral resources of the Republic of South Africa, Coetzee, C.B. (ed), 5th ed., Dept. of mines, Pretoria.

Huffman, R.E., and Davidson, N. (1956) '*Kinetics of the ferrous iron-oxygen reaction in sulphuric acid solution*', J. Am. Chem. Soc., vol. 78, pp. 4836-4842.

Iwai, M., Majima, H. and Awakura, Y. (1982) '*Oxidation of Fe(II) in sulphuric acid solutions with dissolved molecular oxygen*', Metall. Trans. B, vol. 13B, pp. 311-318.

Jan,R.J., Hepworth,M.T., and Fox,V.G., (1976) '*A kinetic study on the pressure leaching of sphalerite*', Met. Trans. B, vol. 7B, pp.353-361.

Keenan, E.A. (1969) '*Bacterial beneficiation of uranium materials*', Ph.D. Thesis, University of New South Wales, in Mathews and Robins (1972) and Chmielewski and Charewicz (1984).

Kortum, (1965) '*Treatise on electrochemistry*', 2nd ed., Elsevier, Amsterdam.

Kuzminkh,I.N. and Yakoutova,E.L. (1950) '*Action of solutions of ferric sulphate on zinc sulphide*' J. Applied Chem. of the U.S.S.R., vol. 23, pp 1197-1202.

Latimer, W.M. (1952) '*Oxidation potentials*', 2nd ed., Prentice Hall, New York.

Levenspiel, O. (1972) '*Chemical Reaction Engineering*', 2nd ed., John Wiley and Sons, New York.

Loveday, B.K., (1975) '*A model for the leaching of non-porous particles*', J. S. Afr. Inst. Min. Met., pp 16-19.

Mathews, C.T., and Robins, R.G. (1972) '*The oxidation of aqueous ferrous sulphate solutions by molecular oxygen*', Proc. Aust. Inst. Min. Met.,no. 242

McAndrew, R.T., Wang, S.S., and Brown, W.R. (1975) '*Precipitation of iron compounds from sulphuric acid leach solutions*', C.I.M. Bulletin, pp. 101-110.

Mizoguchi, T., and Habashi, F. (1981) '*The aqueous oxidation of complex sulphides in hydrochloric acid*', Int. J. Min. Proc., vol. 8, pp. 177-193.

Narita, E., Lawson, F., and Han, K.N. (1983) '*Solubility of oxygen in aqueous electrolyte solutions*', Hydromet., vol. 10, pp. 21-37.

Nattrass, W.A. (1985) Personal Communication, MINTEK.

Naumov,G.B., Ryzhenko,B.N., and Khadakovsky,I.L. (1974) '*Handbook of Thermodynamic data*', U.S. Department of Commerce, National Technical Information Service, U.S. Geological Survey, Menlo Park, California.

Nicol, D.I. (1975) *The oxidation of aqueous solutions of ferrous sulphate in a bubble column*', National Institute for Metallurgy, Randburg, S.A., report no.1711.

Nicol, M.J., Needles, C.R.S., and Finkelstein, N.P. (1975) '*Electrochemical model for the leaching of uranium dioxide: I-acidic media*', Leaching and Reduction in Hydrometallurgy, Burkin, A.R. (ed), Inst. Min. Met., London.

Parker, A.J. Paul, R.L., and Power, G.P. (1981) '*Electrochemistry of the oxidative leaching of copper from chalcopyrite*',

J. Electranl. Chem., Vol. 118, pp.305-316.

Paul, R.L., Nicol, M.J., Diggle, J.W., and Saunders, A.P. (1977) '*The electrochemical behaviour of galena, I. Anodic dissolution*', Electrochemica Acta, vol. 23, pp. 625-633.

Pawlek,F.E. (1969) *Research in pressure leaching*", J.S.Afr. Min.Metall., vol.69, pp 632-654.

Perry and Chilton (1972) '*Chemical Engineers Handbook*', 5th ed., McGraw-Hill Book Co., New York.

Pitzer, K.S., Roy, R.N., and Sylvester, L.F. (1977) '*Thermodynamics of electrolytes. 7. Sulphuric acid*', J. Am. Chem. Soc., pp. 4930-4936.

Rath,P.C., Paramguru,R.K., and Jena, P.K. (1981) ' *Kinetics of dissolution of zinc sulhide in ferric sulphate and ferric chloride media*', Hydromat., vol.6, pp. 219-230

Scott,P.D., and Nicol,M.J., (1978) *The kinetics of the leaching of zinc sulphide concentrates in acid solutions containing ferric sulphate*', National Institute for Metallurgy, Randburg, report no. 1949.

Scott,T.R. and Dyson,N.F. (1968) '*The catalysed oxidation of zinc sulphide under acid pressure leaching conditions*', Trans.Met. Soc.AIME, vol. 242, pp. 1815-1821.

Springer,G. (1970) '*Observations on the electrochemical reactivity of semiconducting materials*' Trans.Inst.Min.Metall., vol 79, pp. c11-c14.

Ting-Po I, and Narcollas, G.H. (1972) *EQUIL - A general computational*

method for the calculation of solution equilibria', Anal. Chem., vol. 44, no. 2, pp. 1940-1950.

Van Niekerk,C.J. and Allen,D.R. (1977) '*The electrolytic extraction of zinc at the Zinc Corporation of S.A. Ltd.*', J. S.Afr.Inst.Min.Metall., pp 146-149

Verbaan,B. (1977) '*A kinetic study of the dissolution of natural and synthetic sphalerite in aqueous sulphuric acid and in acidic ferric sulphate media*', Ph.D. Thesis, University of Natal, Durban.

Verbaan,B. (1980) '*The leaching of sphalerite in acidic ferric sulphate media in the absence of elemental oxygen*', National Institute for metallurgy, Randburg, Report no. 2038.

Verbaan,B. (1981) '*Leaching process for zinc sulphide containing materials*', U.S. Patent 4274931, 23 June, 1981.

Wadsworth,M.E. (1972) '*Advances in the leaching of sulphide minerals*', Minerals Sci. Engng., vol. 4, no. 4, pp.36-47.

Woodcock, J.T. (1961) '*Some aspects of the oxidation of sulphide minerals in aqueous suspension*', Proc. Aust. Inst. Min. Met., no. 198, pp. 47-78.

Yeagar,E. and Salkind,A.J. (1972) '*Techniques of Electrochemistry*', vol. 1, John Wiley and Sons, New York.

APPENDIX A.

Equilibrium constants for the ferric ferrous sulphate complexing reactions.

Equation	Equilibrium constants (after Dry, 1984) 293 - 363 °K
2.23 a	0
2.23 b	exp(33,334 - 7629,9/T)
2.23 c	0
2.23 d	exp(-900,421 + 39110,926/T + 136,626log(T))
2.23 f	10**(3,339 - 337,37/T)
2.23 g	exp(30,692 - 7290,4/T)

The stability constant for equation 2.23 e (that is, for the HSO_4^- specie) is calculated from the correlation given by Pitzer et al (1977).

The stability constant for equation 2.23 h is calculated from the results reported by Naumov, Ryzhenko, and Khadakovsky (1974) who gave a value of 2,38 for pK, and a value of 0,63 +/- 0,02 kcal/mol for ΔH° at zero ionic strength. From the Gibbs-Helmholtz equation:

$$d\ln(K)/dT = \Delta H^\circ/RT^2 \qquad A.1$$

$$K = 10^{2,38}\exp(1,0672 - 318,18/T) \qquad A.2$$

for the stability constant of the specie $ZnSO_4$

APPENDIX B

Shrinking core model derivation, the reduction of ferric ion by non-zinc sulphidic material, and the effect of the ZnO layer on the particle surface.

B.1 Shrinking core model derivation.

The generalised shrinking core expression for a single particle (Levenspiel, 1972) is:

$$\frac{dm}{dt} = - K a \psi \qquad B.1$$

The nomenclature used in this appendix is defined in the text and in the list of nomenclature on page xi. Defining the molar density, P, as:

$$P = m_s/l_s^2 = m/l^3 \qquad B.2$$

where l is defined by l^3 = volume. Re-arranging B.2:

$$l^2 = (m l_s^2/m_s)^{2/3} \qquad B.3$$

Defining the shape factor as:

$$\gamma = a/l^2 \qquad B.4$$

then

$$a = \gamma(m l_s^2/m_s)^{2/3} \qquad B.5$$

Substituting in B.1:

$$\frac{dm}{dt} = - K \gamma (m l_s^3 / m_s)^{2/3} \psi \qquad B.6$$

Now, if F_s is the total initial mass of all sphalerite particles, and M_s is the total initial moles of zinc in all the sphalerite particles, then the number of particles leached is:

$$n = F_s / \rho l_s^3 \qquad B.7$$

where ρ is the mass density. Then

$$M_s = n m_s \qquad B.8$$

The shrinking core model for all the particles in a particular size class is:

$$\frac{dnm}{dt} = - K n \gamma (m l_s^3 / m_s)^{2/3} \psi \qquad B.9$$

where the shape factor is an average shape factor for all the particles.

$$\frac{dM}{dt} = - K n \gamma l_s^2 (M/M_s)^{2/3} \psi \qquad B.10$$

Substituting B.7 into B.10:

$$\frac{dM}{dt} = - K \gamma (F_s / \rho l_s)(M/M_s)^{2/3} \psi \qquad B.11$$

If this includes a particle size distribution $f(l_s)$, then:

$$-\frac{dM}{dt} = K \int_{l_{min}}^{l_{max}} F_s \Psi (M/M_s)^{2/3} / (\rho l_s) \psi f(l_s)\, dl_s \qquad B.13$$

If M, M_s and F_s are function of l_s and the extent of reaction for a particular size fraction is:

$$e(l_s) = M_s(l_s) - M(1) \qquad B.14$$

then

$$\frac{de(l_s)}{dt} = K \Psi \frac{F_s(l_s)}{\rho l_s} (1 - e(l_s)/M_s(l_s))^{2/3} \psi \qquad B.15$$

If $\delta(l_s)$ is the initial mass fraction of zinc material in class l_s, then:

$$M_s(l_s) = \delta(l_s) M_s \qquad B.16$$
$$F_s(l_s) = \delta(l_s) F_s \qquad B.17$$

Substitution of B.16 and B.17 into gives a rate equation for all particles in class l_s.

Using the relation that rates are independent:

$$\Sigma \frac{de(l_{s_i})}{dt} = \frac{d}{dt} \Sigma e(l_{s_i}) \qquad B.18$$

for i size classes, enables the total extent to be calculated. Note that the solutions conditions factor, ψ, is a function of the total extent, which means that this calculation must be performed iteratively. A FORTRAN 77 program was written to calculate this using an I.M.S.L. library

package for stiff differential equations. (refer to Appendix K for program)

B.2 Reduction of ferric ion by non-zinc sulphidic material.

Assuming that the non-zinc sulphidic material reacts at the same rate as the sphalerite and proportional the amount of material present, then:

$$d[Fe(II)]/dt = -\,d[Fe(III)]/dt = 2x0,29\ d[Zn(II)]/dt \qquad B.19$$

where 0,29 is the molar ratio of non-zinc sulphides to zinc sulphide present in the sphalerite. If the sulphidic iron is assumed to be FeS, then this will increase the Fe(II) concentration in solution during leaching in the following manner:

$$d[Fe(II)]/dt = 0,24\ d[Zn(II)]/dt \qquad B.20$$

where 0,24 is the molar ratio of FeS to ZnS present in the sphalerite. The major reduction of ferric ion is due to leaching of sphalerite. The total reduction of ferric ion due to the leaching of zinc, iron and manganese sulphides is:

$$d[Fe(II)]/dt = 2,82\ d[Zn(II)]/dt \qquad B.21$$

$$d[Fe(III)]/dt = -\,2,58\ d[Zn(II)]/dt \qquad B.22$$

where 2,82 is the total molar increase in ferrous ions in solution due to the leaching of the FeS fraction and the reduction of Fe(III), while 2,58 is the total molar reduction of Fe(III) due to the leaching of zinc, iron and manganese sulphides. Using B.21 and B.22 the change in the

solution conditions is calculated at each iteration in the numerical solution of equation B.18.

B.3 Effect of the ZnO reaction.

Sphalerite exposed to the air forms an oxide layer around each particle. It was experimentally demonstrated that the oxide layers of zinc and iron leached very rapidly, even in low concentration of acid. This oxide layer reacts within a few seconds on contact with the leaching solution as follows:

$$ZnO + H_2SO_4 \rightarrow ZnSO_4 + H_2O \qquad B.23$$

$$FeO + H_2SO_4 \rightarrow FeSO_4 + H_2O \qquad B.24$$

The amount of oxide present is determined by leaching the sphalerite with dilute sulphuric acid (0,05 M). These reactions thus alter the solution conditions for the commencement of the sulphide leaching, and this is accounted for by adjusting the initial conditions for the program.

APPENDIX C.

Values for correlation given by Nerita, Lawson and Han (1983)

In section 2.2, the solubility of oxygen in aqueous electrolyte solution is discussed. Nerita, Lawson and Han (1983) presented a semi-empirical correlation for the solubility of oxygen. The constants used for the present system in eqution 2.38 are:

Cation	K_i	Anion	K_i
H^+	0,00	HSO_4^-	0,16
Zn^{2+}	0,27	SO_4^{2-}	0,28
Fe^{3+}	0,25		
Fe^{2+}	0,25		

From an examination of the values for other cations, a value of 0,25 was decided on for the ferric and ferrous ions, based on the charge of these cations.

APPENDIX D

Titration methods for Fe(III) and H_2SO_4 concentration determination.

D.1 Ferric ion determination.

A standard 0,179M sodium thiosulphate solution was prepared. Approximately three drops chloroform and 0,1 g/l $NaCO_3$ was added.
1,0ml 0,179M $Na_2S_2O_3$ = 0,01g Fe(III)

Method.

(i) Add an excess of KI crystals to the solution sample;
(ii) Titrate with the sodium thiosulphate solution until the brown colour turns orange;
(iii) Near the end point the solution becomes pale yellow - additional KI may be dissolved in the solution;
(iv) At the end-point the solution is colourless.

D.2 Sulphuric acid determination.

A standard 0,204 M sodium carbonate solution was prepared and a mixed indicator was used to determine the end-point. This indicator consisted of 0,2g d'methyl yellow and 0,2g methyl blue dissolved in 200ml methanol.

Method.

(i) All ferric ion in solution must be reduced to ferrous ion, i.e. titrate with $Na_2S_2O_3$ (section D.1) first.
(ii) Add 3 drops mixed indicator to the solution, and titrate until the purple colour turns green, indicating the end-point.

APPENDIX E

Raw data for Black Mountain sphalerite by ferric ion in the absence of oxygen.

E.1 Leaching in the pressure reactor.

E.1.1 Initial conditions.

Run	Temp °C	RPM	Fe(III) g/l	Fe(II) g/l	H2SO4 g/l	ZnS g/l	Size µm
28	90	450	19,1	2,78	10,2	20	unscreen
39	80	450	3,50	5,39	10,2	2	unscreen
40	80	450	6,00	2,92	8,2	2	unscreen
42	80	450	8,85	0,03	10,9	2	unscreen
54	50	210	5,713	0,0603	11,85	3	+74 -105
55	50	210	5,675	0,0603	11,80	3	+74 -105
56	50	210	5,560	0,0603	11,95	3	+53 -74
57	50	290	5,675	0,0603	11,80	3	+53 -74
58	50	290	11,575	0,0603	11,85	3	+53 -74
59	90	290	11,575	0,0603	12,10	3	+53 -74
61	50	400	5,675	0,0603	11,70	3	+53 -74
62	50	615	5,663	0,0603	11,50	3	+53 -74
63	90	495	5,675	0,0603	11,60	3	+53 -74

Runs 28, 39, 40, and 42 were conducted in 10l of solution, while runs 54-59 and 61-63 were in 5l of solution. The Eh values were measured with respect to the saturated calomel electrode.

E.1.2 Raw data for leaching in pressure reactor.

All values, except those for conversion, are measured results.

Run 28					
Time min	Zinc g/l	Ferric g/l	X (conv) -	H2SO4 mol/l	Total Fe g/l
0	0,116	19,10	0,00	0,101	21,88
5	2,02	14,90	0,193	-	
20	2,48	13,30	0,336	-	
40	3,17	12,30	0,305	-	
60	3,53	11,70	0,344	-	
120	3,45	10,85	0,378	-	
180	4,17	9,85	0,408	-	
240	4,33	8,80	0,444	-	
300	4,85	8,20	0,476	-	

Run 34					
Time min	Zn(II) mg/l	X (conv) -	Fe(III) g/l	H2SO4 g/l	Eh mV
0	0,00	0,00	5,713	11,85	528
5	37,44	0,0252	5,550	11,40	510
10	52,26	0,0352	5,450	11,45	503
15	60,40	0,0407	5,400	-	497
20	64,3	0,0433	5,575	11,60	496
30	77,2	0,0521	5,550	11,60	491
40	84,5	0,0569	5,538	-	486
50	92,3	0,0621	5,538	-	485
60	98,5	0,0663	5,525	11,70	478

Run 39					
Time min	Zinc g/l	Ferric g/l	X (conv) -	H2SO4 mol/l	Total Fe g/l
0	0,262	3,5	0,000	0,104	8,89
5	0,290	3,4	0,006	0,103	
10	0,350	3,2	0,109	0,103	
15	0,398	3,1	0,147	0,102	
30	0,494	3,0	0,254	0,103	
60	0,508	-	0,268	-	
120	0,578	2,8	0,338	0,104	
180	0,588	2,6	0,348	0,103	
240	0,606	2,69	0,367	0,104	
300	0,626	2,6	0,387	0,102	

Final residue collected: 15,3g

Run 33					
Time min	Zn(II) mg/l	X (conv) -	Fe(III) g/l	H2SO4 g/l	Eh mV
0	0,00	0,00	5,673	11,80	524
5	35,48	0,0229	-	-	506
10	46,3	0,0312	5,600	11,75	501
15	53,1	0,0371	5,573	11,70	498
20	62,3	0,0421	5,600	-	494
30	70,6	0,0475	5,536	11,65	485
40	78,9	0,0531	5,525	-	486
50	84,2	0,0569	5,500	-	485
60	92,3	0,0622	5,523	12,00	483

Run 40					
Time min	Zinc g/l	Ferric g/l	X (conv) -	H2SO4 mol/l	Total Fe g/l
0	0,240	4,00	0,000	0,083	8,92
5	0,254	3,85	0,115	0,084	
10	0,262	3,75	0,143	0,082	
15	0,410	3,65	0,171	0,080	
30	0,442	3,65	0,203	0,083	
60	0,484	3,50	0,244	0,081	
120	0,552	3,40	0,314	0,086	
180	0,564	3,35	0,326	0,082	
240	0,578	3,35	0,354	0,082	
300	0,616	3,25	0,379	0,082	

Final residue collected: 14,5g

Run 36					
Time min	Zn(II) mg/l	X (conv) -	Fe(III) g/l	H2SO4 g/l	Eh mV
0	0,00	0,00	5,650	11,95	528
5	37,28	0,0246	5,513	11,5	495
10	78,7	0,0330	5,488	-	486
15	96,2	0,0662	5,450	-	481
20	110,34	0,0743	5,388	11,40	477
30	144,3	0,0972	5,350	-	471
40	185,13	0,1213	5,263	-	466
50	191,25	0,1288	5,238	11,65	465
60	223,63	0,1316	5,188	11,35	460

Run 42					
Time min	Zinc g/l	Ferric g/l	X (conv) -	H2SO4 mol/l	Total Fe g/l
0	0,242	9,85	0,000	0,111	8,85
5	0,408	8,40	0,167	0,116	
10	0,428	8,10	0,187	0,109	
15	0,434	8,30	0,213	0,114	
30	0,310	8,25	0,270	0,113	
60	0,538	8,00	0,316	0,112	
120	0,594	7,90	0,333	0,110	
180	0,622	7,90	0,383	0,114	
240	0,632	7,80	0,413	-	
300	0,684	6,65	0,443	-	

Final residue collected: 14,4g

Run 57					
Time min	Zn(II) mg/l	X (conv) -	Fe(III) g/l	H2SO4 g/l	Eh mV
0	0,00	0,00	5,675	11,60	527
5	63,14	0,0428	5,513	-	496
10	84,7	0,0597	5,500	11,75	487
15	102,72	0,0692	5,438	-	481
20	120,30	0,0877	5,375	-	476
30	177,60	0,1196	5,313	11,75	469
40	233,80	0,1574	5,238	11,70	464
50	251,80	0,1696	5,163	-	460
60	271,00	0,1833	5,063	11,35	457

Run 58					
Time min	Zn(II) mg/l	X (conv) -	Fe(III) g/l	H2SO4 g/l	Eh mV
0	0,00	0,00	11,226	11,63	526
5	98,2	0,0661	10,950	11,80	506
10	121,2	0,0816	11,068	-	497
15	147,2	0,0991	10,888	-	491
20	184,7	0,1244	10,975	-	487
30	195,0	0,1313	10,822	12,40	480
40	245,0	0,1650	10,738	-	475
50	306,0	0,2067	10,673	12,26	471
60	352,0	0,2370	10,563	12,28	467

Run 59				
Time min	Zn(II) mg/l	X (conv) -	Fe(III) g/l	H2SO4 g/l
0	0,00	0,00	11,375	12,10
5	165,0	0,1110	10,925	-
10	210,0	0,1414	10,825	-
15	240,9	0,1616	10,650	-
20	270,0	0,1816	10,509	-
30	312,0	0,2098	10,313	12,10
40	372,0	0,2210	10,300	-
50	413,0	0,2770	10,225	-
60	424,0	0,2853	10,088	-

Run 61				
Time min	Zn(II) mg/l	X (conv) -	Fe(III) g/l	H2SO4 g/l
0	0,00	0,00	5,675	11,70
5	64,8	0,0436	5,512	-
10	96,75	0,0652	5,475	-
15	126,84	0,0853	5,333	-
20	162,60	0,1230	5,263	-
30	198,54	0,1337	5,138	-
40	236,14	0,1590	5,100	-
50	302,16	0,2035	5,013	-
60	343,12	0,2314	5,000	-

Run 62				
Time min	Zn(II) g/l	X (conv) -	Fe(III) g/l	H2SO4 g/l
0	0,00	0,00	5,663	11,50
5	64,05	0,0430	5,488	-
10	92,05	0,0613	5,463	-
15	122,43	0,0821	5,295	-
20	131,34	0,0884	5,400	-
30	157,35	0,1060	5,350	-
40	186,63	0,1257	5,238	-
50	212,71	0,1432	5,180	-
60	225,15	0,1516	5,063	-

Run 63				
Time min	Zn(II) mg/l	X (conv) -	Fe(III) g/l	H2SO4 g/l
0	0,00	0,00	5,675	11,60
5	135,13	0,091	5,538	-
10	168,45	0,1134	5,275	-
15	190,05	0,1280	5,225	-
20	214,05	0,1441	5,200	-
30	240,10	0,1617	5,138	-
40	251,25	0,1692	5,075	-
50	267,10	0,1801	5,015	-
60	277,75	0,1870	5,000	-

E.2 Leaching results from the constant-temperature bath equipment.

E.2.1 Initial conditions.

All experiments in this section were conduuted at 50°C. The initial Zn concentrations are those measured from the ZnO reaction. The redox potentials, Eh, are measured in mV vs S.C.E.. The size fraction of particles was all the same : -105+74 microns.

Run	Ferric mol/l	Ferrous mol/l	H2SO4 mol/l	Zinc mol/l	ZnS g/l	RPM
F1	0.1065	0.000108	0.100	0.1542 E-03	3.00	800
F2	0.1016	0.000540	0.100	0.1542 E-03	3.00	800
F3	0.1015	0.001079	0.100	0.1542 E-03	3.00	800
F4	0.1030	0.005395	0.100	0.1542 E-03	3.00	800
F5	0.1019	0.01079	0.100	0.1542 E-03	3.00	800
F6	0.1065	0.02877	0.100	0.1542 E-03	3.00	800
F7	0.1077	0.05395	0.100	0.1542 E-03	3.00	800
F8	0.1016	0.10791	0.100	0.1542 E-03	3.00	800
F11	0.3250	0.000108	0.100	0.1542 E-03	3.00	800
F12	0.3244	0.001079	0.100	0 1542 E-03	3.00	800
F13	0.3229	0.005395	0.100	0.1542 E-03	3.00	800
F14	0.3208	0.01079	0.100	0.1542 E-03	3.00	800
F15	0.3103	0.02877	0.100	0.1542 E-03	3.00	800
F16	0.3139	0.05395	0.100	0.1542 E-03	3.00	800
F17	0.3208	0.10790	0.100	0.1542 E-03	3.00	800
F18	0.3236	0.21580	0.100	0.1542 E-03	3.00	800
F19	0.1234	0.000108	0.100	0.1542 E-03	3.00	1350
F20	0.1246	0.02877	0.100	0.1542 E-03	3.00	1350

E.2.2 Raw data.

Run F1

Time min	Zn (meas) mg/l	X (conv)	Eh mV
0.0	10.08	0.00679	409
1.0	17.58	0.01185	377
2.5	18.61	0.01254	375
5.0	26.55	0.01790	369
7.5	29.83	0.02012	364
10.0	34.08	0.02297	360
15.0	42.63	0.02874	352
20.0	48.71	0.03349	344
25.0	60.17	0.04056	344
30.0	69.47	0.04683	340

Run F2

Time min	Zn (meas) mg/l	X (conv)	Eh mV
0.0	10.08	0.00679	378
1.0	13.15	0.00886	366
2.5	15.74	0.01061	362
5.0	19.52	0.01316	359
7.5	20.08	0.01354	355
10.0	24.27	0.01636	352
15.0	29.18	0.02004	348
20.0	39.16	0.02640	343
25.0	43.48	0.02931	342
30.0	50.81	0.03425	338

Run F3

Time min	Zn (meas) mg/l	X (conv)	Eh mV
0.0	10.08	0.00679	360
1.0	7.83	0.00509	355
2.5	16.24	0.01095	350
5.0	19.13	0.01291	347
7.5	24.35	0.01655	344
10.0	29.56	0.01993	343
15.0	31.72	0.02068	340
20.0	38.48	0.02554	338
25.0	42.66	0.02876	336
30.0	46.34	0.03272	334

Run F4

Time min	Zn (meas) mg/l	X (conv)	Eh mV
0.0	10.08	0.00679	316
1.0	13.72	0.00925	314
2.5	17.21	0.01160	311
5.0	21.73	0.01465	312
7.5	26.50	0.01719	312
10.0	27.31	0.01834	311
15.0	29.72	0.02353	310
20.0	36.12	0.02570	309
25.0	45.15	0.03044	308
30.0	50 08	0.03374	308

Run F5

Time min	Zn (meas) mg/l	X (conv)	Eh mV
0.0	10 08	0.00679	496
1.0	12.71	0.00870	498
2.5	15.12	0.01019	494
5.0	17.66	0.01190	494
7.5	24.68	0.01664	493
10.0	28.67	0.01932	493
15.0	33.34	0.02247	492
20.0	38.73	0.02609	492
25.0	39.96	0.02694	492
30.0	42.53	0.02868	492

Run F6

Time min	Zn (meas) mg/l	X (conv)	Eh mV
0.0	10.08	0.00679	467
1.0	10.04	0.00677	467
2.5	12.56	0.00853	467
5.0	17.00	0.01146	467
7.5	18.82	0.01269	467
10.0	20.15	0.01358	463
15.0	29.70	0.02002	467
20.0	32.94	0.02220	467
25.0	36.12	0.02435	467
30.0	40.70	0.02744	467

Run F7

Time min	Zn (meas) mg/l	X (conv)	Eh mV
0.0	10.08	0.00679	447
1.0	9.48	0.00635	447
2.5	10.81	0.00729	447
5.0	14.00	0.00968	447
7.5	19 14	0.01290	447
10.0	23.26	0.01588	447
15.0	29.63	0.01997	447
20.0	33.44	0.02287	447
25.0	37 49	0.02527	447
30.0	41.03	0.02767	447

Run F8

Time min	Zn (meas) mg/l	X (conv)	Eh mV
0 0	10.08	0 00679	423
1 0	9.44	0 00502	423
2 5	11.16	0 00752	423
5.0	14.88	0 01003	423
7.5	19.28	0 01292	423
10.0	22.94	0 01546	423
15.0	27.53	0 01857	423
20.0	32.04	0 02160	423
25.0	29.62	0 02001	423
30.0	46.81	0 03153	423

Run F11

Time min	Zn (meas) mg/l	X (conv)	Eh mV
0.0	10.08	0.00679	628
1.0	9.70	0.00654	607
2.3	11.26	0.00759	596
5.0	13.70	0.00924	590
7.5	17.50	0.01180	583
10.0	19.90	0.01341	581
15.0	23.22	0.01565	578
20.0	29.10	0.01961	574
25.0	30.46	0.02053	571
30.0	37.00	0.02494	569

Run F12

Time min	Zn (meas) mg/l	X (conv)	Eh mV
0.0	10.08	0.00679	582
1.0	9.64	0.00650	575
2.3	12.84	0.00866	573
5.0	17.34	0.01169	570
7.5	18.14	0.01223	568
10.0	21.70	0.01463	566
15.0	28.36	0.01912	564
20.0	31.22	0.02105	562
25.0	36.94	0.02490	560
30.0	41.32	0.02785	558

Run F13

Time min	Zn (meas) mg/l	X (conv)	Eh mV
0.0	10.08	0.00679	540
1.0	9.00	0.00607	539
2.3	10.90	0.00733	538
5.0	13.62	0.00918	537
7.5	17.52	0.01181	536
10.0	23.24	0.01567	536
15.0	29.90	0.02016	536
20.0	30.82	0.02078	535
25.0	36.62	0.02469	535
30.0	41.62	0.02806	535

Run F14

Time min	Zn (meas) mg/l	X (conv)	Eh mV
0.0	10.08	0.00679	520
1.0	8.30	0.00559	520
2.3	11.63	0.00783	520
5.0	13.62	0.00918	520
7.5	17.22	0.01161	520
10.0	23.24	0.01567	520
15.0	29.90	0.02016	519
20.0	30.82	0.02078	519
25.0	36.62	0.02469	518
30.0	42.24	0.02847	518

Run F15

Time min	Zn (meas) mg/l	X (conv)	Eh mV
0.0	10.08	0.00679	494
1.0	8.50	0.00573	493
2.3	11.22	0.00756	493
5.0	15.96	0.01076	493
7.5	20.36	0.01372	493
10.0	24.50	0.01652	493
15.0	28.50	0.01921	493
20.0	33.92	0.02287	493
25.0	38.02	0.02563	492
30.0	43.82	0.02948	492

Run F16

Time min	Zn (meas) mg/l	X (conv)	Eh mV
0.0	10.08	0.00679	474
1.0	7.40	0.00499	474
2.3	10.44	0.00701	473
5.0	14.22	0.00958	473
7.5	18.24	0.01230	473
10.0	24.24	0.01634	473
15.0	29.70	0.02002	473
20.0	32.06	0.02160	473
25.0	37.22	0.02509	473
30.0	42.90	0.02892	473

Run F17

Time min	Zn (meas) mg/l	X (conv)	Eh mV
0.0	10.08	0.00679	452
1.0	6.56	0.00557	451
2.3	10.82	0.00729	451
5.0	15.72	0.01060	451
7.5	19.82	0.01302	451
10.0	22.80	0.01537	451
15.0	28.12	0.01896	451
20.0	31.90	0.02150	451
25.0	38.04	0.02564	451
30.0	41.72	0.02812	451

Run F18

Time min	Zn (meas) mg/l	X (conv)	Eh mV
0.0	10.08	0.00679	427
1.0	8.34	0.00562	427
2.3	11.24	0.00758	427
5.0	14.34	0.00966	427
7.5	20.22	0.01363	427
10.0	24.18	0.01630	427
15.0	28.30	0.01908	427
20.0	32.06	0.02161	427
25.0	38.24	0.02578	427
30.0	42.56	0.02869	427

Run F19			
Time min	Zn (meas) mg/l	X (conv)	Eh mV
0.0	10.08	0.00679	411
1.0	5.44	0.00367	384
2.5	6.50	0.00573	380
5.0	17.48	0.01178	574
7.3	18.34	0.01236	573
10.0	23.72	0.01599	570
13.0	28.10	0.01894	567
20.0	31.92	0.02152	563
25.0	27.10	0.01826	561
30.0	43.34	0.02922	559

Run F20			
Time min	Zn (meas) mg/l	X (conv)	Eh mV
0 0	10.08	0.00679	468
1.0	5.72	0.00386	468
2.5	10.22	0.00729	468
5.0	17.32	0.01168	467
7.5	18.30	0.0.234	467
10.0	23.54	0.01607	467
15.0	28.16	0.01930	467
20.0	32.04	0.02195	467
25.0	38.24	0.02575	467
30.0	49.00	0.03363	467

APPENDIX F

Raw data for the ferrous ion oxidation runs.

F.1 Initial conditions.

Run	Temp K	Ferric g/l	Tot. Fe g/l	Acid mol/l	Press bar
2	363.	0.400	8.761	0.382	4.5
4	363.	0.600	11.118	0.100	5.0
7	363.	0.300	19.802	0.200	4.5
10	363.	1.200	18.654	0.200	4.5
11	363.	0.100	19.636	0.500	4.5
13	363.	0.400	11.761	0.500	5.0
17	363.	0.300	19.752	0.500	4.5
27	363.	0.400	20.840	0.500	4.5
32	353.	5.100	21.650	0.500	4.5
35	353.	1.100	21.991	0.500	3.0
21	343.	0.300	20.829	0.500	4.5
23	343.	0.200	20.840	0.500	4.5
25	343.	0.300	20.829	0.500	4.5
31	343.	0.700	21.238	0.500	4.5
33	343.	1.300	21.749	0.500	2.0
34	333.	1.150	21.958	0.500	1.0
51	321.	0.300	19.730	0.510	3.0

All runs were conducted at a stirrer speed of 450 RPM.

F.2 Measured results for the ferrous ion oxidation runs.

Run 2

Time min	Ferric g/l	l/Ferrous l/mol	Conversion -
0.	0.40	6.658	0.0000
10.	0.80	6.991	0.0477
20.	1.60	7.660	0.1193
30.	1.93	8.168	0.1849
40.	2.25	8.544	0.2207
50.	2.35	8.677	0.2327
60.	3.00	9.832	0.3102
70.	3.25	10.068	0.3460
80.	3.50	10.566	0.3699
90.	4.60	13.346	0.5011

Run 4

Time min	Ferric g/l	l/Ferrous l/mol	Conversion -
0.	0.60	3.305	0.0000
17.	4.60	8.361	0.3803
27.	6.10	11.120	0.5229
37.	6.80	12.922	0.5894
47.	7.35	15.638	0.6608
57.	7.95	17.613	0.6988
67.	8.40	20.529	0.7416
97.	8.80	24.071	0.7795
107.	9.00	26.344	0.7986
117.	9.00	26.344	0.7986

Run 7

Time min	Ferric g/l	l/Ferrous l/mol	Conversion -
0.	0.30	2.861	0.0000
10.	0.15	4.087	0.3000
20.	9.80	5.579	0.4871
30.	11.60	6.803	0.5794
40.	12.15	7.292	0.6076
50.	14.25	10.030	0.7153
60.	14.30	10.224	0.7281
70.	14.90	11.351	0.7486
80.	15.10	11.857	0.7589

Run 10

Time min	Ferric g/l	l/Ferrous l/mol	Conversion -
0.	1.20	3.197	0.0000
10.	3.35	3.896	0.1346
20.	5.50	4.391	0.3037
30.	9.80	6.162	0.4813
41.	11.70	8.024	0.6016
51.	12.20	8.665	0.6302
61.	13.00	9.868	0.6761
71.	13.80	11.040	0.7104
80.	14.20	12.327	0.7448

Run 11

Time min	Ferric g/l	l/Ferrous l/mol	Conversion -
0.	0.10	2.656	0.0000
10.	7.05	4.454	0.3538
20.	10.05	5.871	0.5092
30.	11.65	6.968	0.5912
40.	12.30	7.607	0.6345
50.	13.30	8.807	0.6757
60.	14.10	10.068	0.7166
70.	14.60	11.081	0.7422
80.	14.90	11.783	0.7576
90.	15.20	12.580	0.7729
127.	15.60	13.827	0.7924

Run 13

Time min	Ferric g/l	l/Ferrous l/mol	Conversion -
0.	0.40	4.912	0.0000
10.	1.25	5.867	0.1628
20.	3.50	6.755	0.2739
30.	4.45	7.632	0.3565
40.	3.25	8.370	0.4269
50.	3.65	9.133	0.4621
60.	6.05	9.771	0.4973
70.	6.30	10.218	0.5193
80.	6.60	10.812	0.5437
90.	7.30	13.096	0.6230

Run 23

Time min	Ferric g/l	1/Ferrous l/mol	Conversion -
0.	0.20	2.703	0.0000
5.	1.30	2.836	0.0533
10.	2.40	3.026	0.1066
20.	3.90	3.294	0.1793
30.	5.25	3.579	0.2447
40.	6.65	3.932	0.3123
50.	7.85	4.295	0.3706
60.	8.80	4.634	0.4167
75.	9.70	5.009	0.4603
90.	10.75	5.530	0.5111
105.	11.40	5.911	0.5426

Run 25

Time min	Ferric g/l	1/Ferrous l/mol	Conversion -
0.	0.30	2.718	0.0000
5.	1.70	2.917	0.0682
10.	2.90	3.112	0.1267
20.	3.90	3.296	0.1734
31.	6.60	3.922	0.3069
35.	6.90	4.006	0.3215
40.	7.30	4.186	0.3507
50.	8.40	4.479	0.3946
60.	9.10	4.758	0.4287
75.	9.80	5.106	0.4676
90.	10.75	5.536	0.5090
105.	11.15	5.765	0.5285

Run 21

Time min	Ferric g/l	1/Ferrous l/mol	Conversion -
0.	0.30	2.715	0.0000
5.	1.20	2.845	0.0438
10.	2.18	2.987	0.0901
20.	3.65	3.246	0.1622
30.	5.20	3.570	0.2267
40.	6.20	3.814	0.2674
50.	7.35	4.108	0.3434
60.	8.25	4.436	0.3823
75.	9.30	4.840	0.4284
90.	10.70	5.509	0.5066
105.	11.10	5.736	0.5261

Run 17

Time min	Ferric g/l	1/Ferrous l/mol	Conversion -
0.	0.20	2.869	0.0000
10.	6.10	4.087	0.2982
19.	7.40	4.592	0.3753
30.	9.80	5.607	0.4864
40.	11.10	6.449	0.5532
50.	12.30	7.285	0.6272
60.	13.10	8.389	0.6580
75.	13.90	9.535	0.6992
90.	14.60	10.831	0.7351

Run 27

Time min	Ferric g/l	1/Ferrous l/mol	Conversion -
0.	0.40	2.720	0.0000
15.	4.75	3.468	0.2118
45.	12.00	6.313	0.3675
60.	13.80	7.927	0.4556
120.	17.15	15.124	0.8193
180.	17.40	16.223	0.8717
240.	19.00	30.324	0.9100

Run 31

Time min	Ferric g/l	1/Ferrous l/mol	Conversion -
0.	0.70	2.717	0.0000
5.	1.90	2.885	0.0367
10.	3.93	3.228	0.1335
30.	6.40	3.761	0.2693
60.	10.30	5.010	0.4441
90.	11.90	5.720	0.5102
180.	14.30	8.041	0.6421
240.	15.25	9.218	0.6873

Run 32

Time min	Ferric g/l	1/Ferrous l/mol	Conversion -
0.	3.10	3.372	0.0000
5.	6.40	3.659	0.0785
10.	7.43	3.930	0.1420
15.	8.25	4.196	0.1964
30.	11.30	5.391	0.3746
60.	12.10	5.863	0.4220
120.	13.43	9.000	0.6234
180.	14.35	10.529	0.6797
240.	17.20	12.340	0.7213

Run 33

Time min	Ferric g/l	1/Ferrous l/mol	Conversion -
0.	1.30	2.729	0.0000
5.	1.90	2.813	0.0292
10.	2.40	2.884	0.0538
15.	3.03	2.964	0.0816
30.	4.35	3.244	0.1389
60.	6.60	3.683	0.2192
120.	9.20	4.447	0.3863
180.	11.10	5.240	0.4792
240.	12.60	5.968	0.5428
300.	13.13	6.489	0.5795

Run 35

Time min	Ferric g/l	1/Ferrous l/mol	Conversion -
0.	1.30	2.671	0.0000
5.	2.80	2.908	0.0814
10.	4.40	3.172	0.1580
15.	5.80	3.446	0.2250
30.	8.35	4.091	0.3470
60.	11.00	5.077	0.4723
120.	13.90	6.896	0.6127
180.	15.10	8.097	0.6701
240.	16.10	9.472	0.7180
300.	16.15	9.553	0.7204

Run 34

Time min	Ferric g/l	1/Ferrous l/mol	Conversion -
0.	1.15	2.682	0.0000
5.	1.20	2.688	0.0024
10.	1.43	2.721	0.0144
15.	1.60	2.741	0.0216
30.	2.10	2.810	0.0457
60.	3.10	2.959	0.0937
120.	4.30	3.196	0.1610
180.	5.85	3.464	0.2339
240.	6.80	3.683	0.2715

Run 51

Time min	Ferric g/l	1/Ferrous l/mol	Conversion -
0.	0.30	2.872	0.0000
5.	0.50	2.902	0.0102
10.	0.65	2.923	0.0180
15.	0.90	2.963	0.0309
20.	1.13	3.003	0.0437
30.	1.35	3.036	0.0548
40.	1.50	3.061	0.0618
50.	1.80	3.112	0.0771
60.	2.13	3.174	0.0932

APPENDIX G

Leaching of Black Mountain sphalerite in acidic ferric sulphate media in the presence of oxygen.

G.1 Initial conditions.

Run	Temp °C	RPM	Fe(III) g/l	Fe(II) g/l	H2SO4 g/l	ZnS g/l	Size µm	$p(O_2)$ bar
44	80	450	7,35	1,93	12,35	5	full	0,5
60	90	465	11,465	0,0602	12,1	9	+53-74	3
64	90	465	5,35	0,0602	11,8	16	+53-74	2

Run 44

Time min	Zn(II) g/l	Fe(III) g/l	H2SO4 g/l	X (conv) -
0	0,011	7,35	12,35	0,00
5	0,121	6,75	12,20	0,056
10	0,361	6,30	12,25	0,164
15	0,481	6,10	12,10	0,189
30	0,657	6,00	12,05	0,260
60	0,853	6,00	12,70	0,359
120	1,006	5,70	11,60	0,401
180	1,071	5,35	11,40	0,427
240	1,122	5,70	11,10	0,448
300	1,138	5,90	11,25	0,454

Run 64

Time min	Zn(II) g/l	Fe(III) g/l	X (conv) -
0	0,00	5,350	0,00
5	1,002	3,200	0,126
10	1,650	2,200	0,208
15	1,800	1,738	0,227
20	1,984	1,538	0,250
25	2,104	1,413	0,265
40	2,230	1,313	0,281
50	2,416	1,168	0,304
60	2,580	1,400	0,321
70	2,720	1,525	0,342
80	2,870	1,625	0,361
90	3,010	1,688	0,379
100	3,030	1,763	0,381
110	3,130	1,863	0,397
120	3,330	1,975	0,407

Run 60

Time min	Zn(II) g/l	Fe(III) g/l	X (conv) -
0	0,00	11,465	0,00
5	0,093	9,250	0,012
10	0,850	8,875	0,108
15	1,008	8,500	0,223
20	1,130	8,400	0,253
30	1,296	8,038	0,288
40	1,450	7,938	0,325
50	1,800	7,888	0,336
60	1,670	7,838	0,374
70	1,684	7,825	0,377
80	1,700	7,825	0,380
90	1,816	7,888	0,406
100	1,870	7,875	0,419
110	1,900	7,913	0,425

APPENDIX H

Experimental results for the determination of the oxide layers on the surface of the sphalerite particles.

The amount of oxide present on the solid surface is obtained by leaching the sphalerite in dilute sulphuric acid (0,05M). Refer to section 2.1.3.

H.1 Initial conditions.

Run	Mass Zn g	H2SO4 mol/l	Temp °C	% Zn as oxide	% Fe as oxide	Size range (microns)
	1,3677	0,01448	48	1,767	33,37	full
	1,3809	0,01571	48	1,262	21,89	full
	1,2291	0,03011	48	1,311	22,87	ful'
	3,0000	0,10000	48	0,677	-	-10!

H.2 Concentration data

Time min	Zn B1 g/l	Zn B2 g/l	Zn B3 g/l	Zn B4 g/l
0	0,00105	0,00040	0,00025	0,0000
1	"	"	"	0,01008
2,5	0,01300	0,00700	0,0067	0,01015
5	0,01005	0,00750	0,01635	0,01040
7,5	"	"	"	0,01055
10	0,01005	0,00805	0,00680	0,01060
15	0,01775	0,00785	0,00710	"
25	0,01305	0,00825	0,00825	"

These results indicate that for the unscreened sample only 1,2% of the total Zn is in the oxide form. For the size fraction -105 +74 µm the comparable figure is 0,6% Zn. This is a very low figure compared to the Gamsberg sphalerite for which 8,3% of the zinc was in the oxide form.

APPENDIX I

Analysis of Gamsberg sphalerite leaching data in the absence of oxygen.

I.1 Calculation of the minimum sum of squares error.

The leaching of Gamsberg sphalerite was analysed in section 4.2 in terms of an electrochemical shrinking core model derived in section 2.1.3. This model has the parameters k' and K. Refer to section 4.2. Table I.1 represents sum of squares calculated at constant k' by golden section search. Refer to section 4.2. A slice through the sum of squares surface is shown in figure I.1, indicating that in the K-direction the minimum is well-defined.

I.2 Calculation of the activation energy for Gamsberg sphalerite.

Table I.2 represents the rate data at different temperatures, from which the activation energy has been calculated. These results have been plotted in the Arrenhius form as figure I.2. From this the activation energy has been determined as 79,8 kJ/mol.

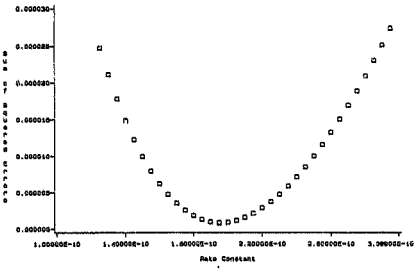

Figure I.1 Slice through the sum of squares plot for constant k (k=17,3) From this it can be seen that the minimum is well defined.

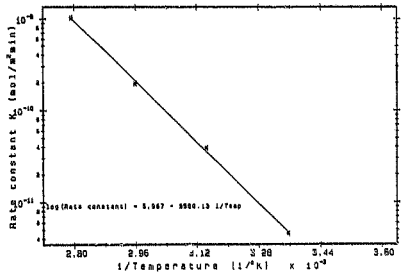

Figure I.2 Arrenhius diagram for Gamsberg sphalerite. Data from table I.2.

Table I.1 Calculation of the minimum sum of squared errors for values of parameter k' for Gamsberg leaching data.

k'	K	Squared errors
V^{-1}	mol/m^2min	-
16,4	0,3814	0,9489
16,5	0,3542	0,9289
16,6	0,3288	0,9115
16,7	0,3054	0,8965
16,8	0,2835	0,8841
16,9	0,2632	0,8743
17,0	0,2444	0,8668
17,1	0,2269	0,8617
17,2	0,2107	0,8590
17,3	0,1956	0,8587
17,4	0,1816	0,8608
17,5	0,1686	0,8651
17,6	0,1565	0,8717
17,7	0,1454	0,8807
17,8	0,1349	0,8919
17,9	0,1253	0,9052
18,0	0,1163	0,9208

Table I.2 Calculation of the dependance of rate on temperature Gamsberg leaching data.

Temp	k'	K
°C	V^{-1}	mol/m^2min
25	19,62	$0,4545 \times 10^{-11}$
45	18,39	$0,3888 \times 10^{-10}$
85	16,33	$0,1033 \times 10^{-8}$

APPENDIX J

Estimation of the parameters for the Fe(II) oxidation reaction.

J.1 Second order rate constant.

The ferrous ion oxidation reaction is assumed to be second order in ferrous ion concentration, and first order in oxygen. Plotting 1/[Fe(II)] against time, k, the apparent rate constant, can be determined from the slope, and the effect of mass-transfer can be determined. If the slope of the second order rate plot is curved and not straight in the initial part of the reaction, then mass-transfer plays a significant role. Examination of these plots indicates that mass-transfer is not a rate controlling step. The slopes of these graphs are presented in Table J.1. Figure J.1 indicates the reproducibility of these results.

J.2 Calculation of oxygen concentration.

The solubility of oxygen in pure water can be determined from the Henry's law constant, H, given Perry (1972). The oxygen concentration in an electrolyte solution is calculated from the correlation given by Narita, Lawson and Han (1983), equation 2.38. Atmospheric pressure was measured

Table J.1 Calculation of k, $[O_2]$ and $[H^+]$

Run	Temp	k	$[O_2]$	$[H^+]$
	°C		mol/l	mol/l
2	363	0,0603	0,269	2,644
4	363	0,1868	0,302	0,164
7	363	0,1337	0,259	0,252
11	363	0,1150	0,258	0,414
10	363	0,1201	0,251	0,294
13	363	0,0860	0,295	0,963
17	363	0,0879	0,258	0,415
27	363	0,1052	0,256	0,379
33	343	0,0173	0,167	0,599
32	353	0,0674	0,281	0,561
31	353	0,0476	0,202	0,456
34	333	0,0045	0,121	0,764
21	343	0,0296	0,316	0,612
23	343	0,0335	0,316	0,610
25	343	0,0299	0,316	0,612

at an average value of 83,5 kPa. The concentration of the various ionic species required by the Narita, Lawson and Han correlation are calculated by program EQUIL. The oxygen concentrations calculated for each run are presented in Table J.1.

J.3 Calculation of the hydrogen ion concentration.

The concentration of the hydrogen is not directly measured in that only titrations for total sulphuric acid were made. The concentration of hydrogen ion is calculated by the program EQUIL from the solution

equilibria. The calculated hydrogen ion concentrations are presented in Table J.1

J.4 Dependence of the rate on the hydrogen concentration.

The values for $k/[O_2]$ are plotted against the calculated $[H^+]$ values for the runs at 363K on a log-log plot. These results are presented in Table J.2.

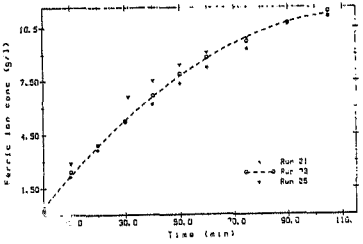

Figure J.1 Reproducibility of ferrous ion oxidation results. Runs 21, 23, 25.

J.5 Calculation of the activation energy.

The values for $k[H^+]^{0,35}/[O_2]$ are plotted on an Arrenhius diagram in section 5.3. These values are presented in Table J.3.

Table J.2 Dependance of the Fe(II) oxidation rate on $[H^+]$

Run	k	Oxygen conc x 10^2	Hydrogen cnc x 10	d
2	0,0603	0,269	2,64	22,4
4	0,0187	0,302	0,164	61,9
7	0,1337	0,259	0,252	51,6
11	0,1150	0,258	0,414	40,7
10	0,1201	0,261	0,295	46,1
13	0,0859	0,296	0,963	29,1
17	0,0879	0,258	0,415	34,1
27	0,1052	0,256	0,380	41,1

where $d = k/[O_2]$

Table J.3 Dependance of Fe(II) oxidation on temperature.

Run	Temp °K	k	$\mathcal{Z}$ x 10^2	$\mathcal{V}$
2	363	0,0603	0,435	13,9
4	363	0,0187	1,33	14,1
7	363	0,1337	0,974	13,7
11	363	0,1150	0,812	14,2
10	363	0,1201	0,927	13,0
13	363	0,0859	0,687	12,5
17	363	0,0879	0.811	10,8
27	363	0,1052	0,832	12,7
33	343	0,0172	0,460	3,76
32	353	0,0674	0,794	8,48
35	353	0,0475	0,616	7,73
34	333	0,0446	0,305	1,46
21	343	0,0296	0,865	3,43
23	343	0,0335	0,866	3,87
25	343	0,0299	0.865	3,46

$\mathcal{Z} = [O_2]/[H^+]^{0,35}$

$\mathcal{V} = k[H^+]^{0,35}/[O_2]$

APPENDIX K

FORTRAN 77 computer program for the calculation of the redox potential, and the simulation of the leaching rate, as discussed in chapter 2.

K.1 Algorithm.

The main program initialises the program, and calls an optimisation routine from the I.M.S.L library to minimise the sum of squared errors. The optimisation program ZXMIN minimises the sum of squared errors calculated in the subroutine OBJECT for both parameters k' and K. When ZXGSN, a golden search optimisation technique is used, then the parameter k' is kept constant, and the optimal K is found.

The subroutine OBJECT calculates the sum of squared differences between the measured data and the simulated leach run for a particular combination of parameters k' and K. The differential equations describing the leaching kinetics are solved using the I.M.S.L. program DGEAR, for which the differential equations are described in subroutine DIF. These equations are presented in section 2.1.3, and Appendix B.

The simulation of the leaching kinetics requires an estimation or prediction of the redox potential. The redox potential, Eh, is calculated in subroutine EQUIL, as discussed in section 2.1. The lay-out and operation of this program is the same as that discussed by Ting-Po and Narcollas (1972) and further inquiry should be directed to that reference before examining EQUIL.

K.2 PROGRAM MAIN

```
      IMPLICIT REAL*8 (A-H),REAL*8 (O-Z)
      REAL*8 KO,MO,K,C(100,3),Y(101),XTC(5),H(3),G(2),W(6),PARS(3)
      EXTERNAL OBJECT
      EXTERNAL SOFSQS
      CHARACTER*15 RUNID
      COMMON /DATA/ TIME(20,15),ZDATA(20,15),FDATA(20,15),FDATA2(20,15)
      COMMON /DATA/ ZSIGMA,FSIGMA,YMAT(10,101),CMAT(10,100,3),TMP(15)
      COMMON /DATA/ NSWCH(15),NPOINT(15)
      COMMON /INITL/ TCINIT(15,5),TC(5),AREA(15),O2S,AMO(15),NEXP
      COMMON /EQUILB/ EQ(8),A,B
      COMMON /EQOXLC/ Z(10),AO(10),OHM(10)
      COMMON TEMP
      COMMON /END/ NEND
      COMMON /PAR/ PAR(2)
      NEND=0
"
" Read in the initial conditions and the measured data
"
      DO 10 I1=1,10
10    READ(2,*)Z(I1),AO(I1),OHM(I1)
      READ(2,*)KO,O2S,VOL
      READ(3,*)NEXP
      READ(3,*)NPOINT(1)
      READ(3,*)(TIME(1,IB),IB=1,NPOINT(1))
      DO 50 I=1,NEXP
       NPOINT(I)=NPOINT(1)
"     AMO(I)=5.DO*200.DO*0.509DO/65.38DO*(1DO-0.083DO)
      AMO(I)=3.DO*0.4965DO/65.38DO-10.08D-3
      TMP(I)=273.DO+50.DO
11    FORMAT(A15)
      DO 12 ID=1,NPOINT(I)
12     TIME(I,ID)=TIME(1,ID)
      READ(3,11)RUNID
      READ(3,*)(ZDATA(I,IA),IA=1,NPOINT(I))
"     READ(3,*)(FDATA(I,IA),IA=1,NPOINT(I))
"     READ(3,*)(FDATA2(I,IA),IA=1,NPOINT(I))
      READ(3,*)(TCINIT(I,IC),IC=1,5)
      NSKIP=1
      IF (NSKIP.EQ.0) THEN
      WRITE(10,1000)RUNID
1000  FORMAT('.bx off',/,'.sp2',/,'.bx 4 35',/,5X,'Run ',A15,-
     /,'.bx 4 12 24 35',-
     /,5X,'Time',4X,'Zn (meas)',4X,'X (conv)',-
     /,5X,'min',5X,'g/lx10^'-
     /,'.bx')
      DO 1001 IZZ=1,NPOINT(I)
      CONV=ZDATA(I,IZZ)*1.D-3/0.02269DO/65.38
1001  WRITE(10,1002)TIME(1,IZZ),ZDATA(I,IZZ),CONV
      END IF
50    CONTINUE
1002  FORMAT(5X,F4.1,3X,F6.2,3X,F12.5)
```

```
"      WRITE(10,1003)
"1003  FORMAT('.bx off',/,'.sp2',/,'.bx 4
"      DO 51 KAK=1,NEXP
"51     WRITE(10,1004)RUNID,TCINIT(KAK,1),TCINIT(KAK,2),TCINIT(KAK,3),-
"         TCINIT(KAK,5)
"1004  FORMAT(5X,A15,2F12.6,F7.3,E16.7)
"
" Calculate spline to fit the extent vs potential data
"
      IF (NSKIP.EQ.0) GO TO 120
      DO 300 I1=1,NEXP
       TEMP=TMP(I1)
       XMO=AMO(I1)
       CALL EQCNST (TEMP,EQ,A,B)
       DO 101 J1=1,5
        TC(J1)=TCINIT(I1,J1)
101     XTC(J1)=TCINIT(I1,J1)
       CALL SPLINE (XTC,TC,Y,C,XMO)
      DO 220 J3=1,100
      YMAT(I1,J3)=Y(J3)
      DO 220 J4=1,4
220   CMAT(I1,J3,J4)=C(J3,J4)
      YMAT(I1,101)=Y(101)
300   CONTINUE
"
" PROGRAM TO FIND PARAMETERS USING NEWTON-RAPHSON METHOD
" ======================================================
"
"
      ZSIGMA=2.D0
      FSIGMA=2.D0
      NPAR=2
      NITER=0
"
" Set initial guesses for parameters
" ORDER IS K, (k1A/k1C), and gamma
      READ(4,*)(PAR(JJ),JJ=1,NPAR)
"     CALL OBJECT (NPAR,PARS,SUMSQS)
"     CALL ZXMIN (OBJECT,NPAR,7,1000,3,PARS,H,G,SUMSQS,W,IER)
      READ(4,*)A,B
      TOL=1.D5
      CALL ZXGSN (SOFSQS,A,B,TOL,XMIN,IER)
      NEND=1
      END=SOFSQS(XMIN)
      WRITE(12,*)XMIN
      WRITE(13,*)XMIN
"      PAR(1)=0.1D12
"      DO 44 IT=1,40
"      PAR(2)=1.73
"       DO 43 IO=1,40
"      F=SOFSQS(PAR(2))
"43    PAR(2)=PAR(2)+0.0025
"44    PAR(1)=PAR(1)+0.005D12
"
```

```
"
120   STOP
      END
```

K.3 FUNCT ON SOFSQS(X)

```
      IMPLICIT REAL*8 (A-H),REAL*8 (O-Z)
      COMMON /PAR/ PAR(2)
      DIMENSION PARS(2)
      PARS(1)=X
      PARS(2)=PAR(2)
      NPAR=2
      CALL OBJECT (NPAR,PARS,SUMSQS)
      SOFSQS=SUMSQS
      RETURN
      END
"
" SUBROUTINE TO CALCULATE SUM OF SQUARES
" ---------------------------------------
```

K.4 SUBROUTINE OBJECT(NPAR,PARS,SUMSQS)

```
      IMPLICIT REAL*8 (A-H),REAL*8 (O-Z)
      EXTERNAL DIFF,FJ
      DIMENSION IWK(12),WK(205),EXTENT(12),WKAREA(40),PARS(2)
      COMMON /DATA/ TIME(20,15),ZDATA(20,15),PDATA(20,15),PDATA2(20,15)
      COMMON /DATA/ ZSIGMA,PSIGMA,YMAT(10,101),CMAT(10,100,3),TMP(15)
      COMMON /DATA/ NSWCH(15),NPOINT(15)
      COMMON /INITL/ TCINIT(15,5),TC(5),AREA(15),O2S,AMO(15),NEXP
      COMMON /PARMS/ DPAR(5),Y(101),C(100,3),N1,NEQUIL
      COMMON /POT/ EH
      COMMON /ERR/ ATC(5)
      COMMON TEMP
      COMMON /END/ NEND
"
" Initialize variables
      DPAR(1)=PARS(1)*1.D-21
      DPAR(2)=PARS(2)*1.D-2
      IF (PARS(1).LT.0.0D0) THEN
        SUMSQS=200
        RETURN
      END IF
"     DPAR(3)=PARS(3)*1.D-1
"
      VOL=1.D0
      TOL=1.0D-10
      METH=2
      MITER=0
```

```
      SSEZ=0.D0
      SSEF1=0.D0
      SSEF2=0.D0
      DO 238 N1=1,NEXP
       DO 203 JA=1,100
        Y(JA)=YMAT(N1,JA)
        DO 203 JB=1,3
203       C(JA,JB)=CMAT(N1,JA,JB)
        Y(101)=YMAT(N1,101)
" Solve differential equations at time of experimental readings
        TEMP=TMP(N1)
        H=1.0D-12
208     INDEX=1
" Set initial conditions
        DO 210 JJ=1,12
210       EXTENT(JJ)=0.D0
        TR=(EXTENT(1)/VOL+TCINIT(N1,5))
        TF=ZDATA(N1,1)/65.38D0*1.D-3
        TE=TCINIT(N1,1)
        TEE=FDATA(N1,1)/55.8D0
"       TF2=FDATA2(N1,1)/55.8D0
        BTIME=0.D0
        NEQUIL=1
        IF (NEND.EQ.1) WRITE(12,219)BTIME,TF,TR,Y(1)
"       IF (NEND.EQ.1) WRITE(12,*)TEE,TE
"       IF (NEND.EQ.1) WRITE(12,*)TF2,TCINIT(N1,2)
        DO 220 M=1,NPOINT(N1)-1
           CALL DGEAR(1,DIFF,FJ,BTIME,H,EXTENT,TIME(N1,M+1),TOL,METH,-
             MITER,INDEX,IWK,WK,IER)
             NEQUIL=2
           IF (IER.EQ.132) THEN
             TOL=1.0D-14
             H=1.0D-15
             GO TO 208
           END IF
        TR=(EXTENT(1)/VOL+TCINIT(N1,5))
        TF=ZDATA(N1,M+1)/65.38D0*1.D-3
"       TE=ATC(1)
        TEE=FDATA(N1,M+1)/55.8D0
"       TF2=FDATA2(N1,M+1)/55.8D0
      IF (NEND.EQ.1) WRITE(12,219)TIME(N1,M+1),TF,TR,EM
"     IF (NEND.EQ.1) WRITE(12,*)TEE,TE
"     IF (NEND.EQ.1) WRITE(12,*)TF2,ATC(2)
"     WRITE(12,*)TC(1),TC(2),TC(3)
219   FORMAT(5X,F6.2,2X,E14.7,2X,E14.7,2X,F8.3)
220      SSEZ=SSEZ+(DABS(EXTENT(1)/VOL+-
                         TCINIT(N1,5)-ZDATA(N1,M+1)*1.D-3/65.38D0))**2
"        SSEF1=SSEF1+(DABS(ATC(1)-FDATA(N1,M+1)/55.8D0))**2
"        SSEF2=SSEF2+(DABS(ATC(2)-FDATA2(N1,M+1)/55.8D0))**2
238   CONTINUE
"
      SUMSQS=SSEZ+SSEF1+SSEF2
"     TKJ=DLOG10(PARS(1))
      TKJ=PARS(1)*1.D-21
```

```
      WRITE(13,240)TKJ,PARS(2),SUMSQS
      WRITE(12,240)TKJ,PARS(2),SUMSQS
240   FORMAT(2X,E14.8,3X,E13 7,3X,E13.7)
      RETURN
      END
"
" Subroutine containing model differential equations
" ___________________________________________________
```

K.5 SUBROUTINE DIFF (N,T,EXTENT,EPRIME)

```
      IMPLICIT REAL*8 (A-H),REAL*8 (O-Z)
      REAL*8 EPRIME(N),EXTENT(N),FC(10),A(11),B(11),LO(11),AB(12)
      REAL*8 K(10)
      DATA A/0.0074,0.0426,0.802,0.1274,.1144,.1031,.1028,.1078,.0813,-
        0.0584,.1746/
      DATA B/.485,.494,.495,.495,.488,.486,.511,.514,.525,.535,.429/
      DATA LO/178.3,126.9,89.16,63.05,44.88,33.66,26.51,19.77,-
        13.95,9.905,4.087/
      COMMON /INITL/ TCINIT(15,5),TC(5),AREA(15),O2S,AMO(15),NEXP
      COMMON /PARMS/ PARS(5),Y(101),C(100,3),NO,NEQUIL
      COMMON /FERR/ ATC(5)
      COMMON /POT/ E
      COMMON TEMP
"
"     VOL=1.D0
"     Calculate redox potentials from spline fit
      I=IDINT(EXTENT(1)/AMO(NO)/0.0100D0+1)
      X=(I-1)*AMO(NO)*0.0100D0
      D=EXTENT(1)-X
"     For calculation of leaching and oxidation results
"     ATC(1)=TCINIT(NO,1)-2.46D0*EXTENT(1)/VOL+EXTENT(2)
"     ATC(2)=TCINIT(NO,2)+2.67D0*EXTENT(1)/VOL-EXTENT(2)
"     ATC(3)=TCINIT(NO,3)-EXTENT(2)
"     ATC(5)=TCINIT(NO,5)+EXTENT(1)/VOL
"     IF (A    ).LT.1.D-6) ATC(1)=DABS(1.D-6)
"     CALL    L(ATC,K,E,EDIFF,NEQUIL)
"     O2S=1.  8D-3*116.D0/101.325D0*DEXP(1936/TEMP-4.48D0)
"     O2S=O2S*DEXP(-(K(5)*0.25D0+(ATC(1)+ATC(2))*0.26D0+K(4)*0.28D0-
          +K(9)*0.16D0))
      IRUN=2
      E=((C(I,3)*D+C(I,2))*D+C(I,1))*D+Y(I)
      IF (IRUN.EQ.42) THEN
        EPRIME(1)=0.D0
        DO 19 JI=2,12
        AB(JI)=20.D0*A(JI-1)*B(JI-1)/65.3800
        IF ((1.D0-EXTENT(JI)/AB(JI)).LT.1.D-12) THEN
          EXTENT(JI)=DABS((1.D0-1.D-12)*B(JI))
        ELSE
          EPRIME(JI)=PARS(1)*20.D0*A(JI-1)*
             (DABS(1.D0-EXTENT(JI)/AB(JI)))**(2.D0/3.D0)*-
```

```
            DEXP(E*PARS(2))/(LO(JI-1)*1.D-6)
          END IF
          EPRIME(1)=EPRIME(1)+EPRIME(JI)
19        CONTINUE
          ELSE
"           IF ((1.D0-EXTENT(1)/AM0(N0)).LT.1.D-6) THEN
"             EXTENT(1)=DABS((1-1.D-6)*AM0(N0))
"           END IF
            EPRIME(1)=PARS(1)*DEXP(PARS(2)*E)*w-
             (1.D0-EXTENT(1)/AM0(N0))**(2.D0/3.D0)
          END IF
"         EPRIME(2)=1.248D+11*(ATC(2)**2)*02S/(K(3)**0.35D0)-
"           *DEXP(-68600.D0/8.314D0/363 D0)
          RETURN
          END
"
" Dummy subroutine used by DGEAR
" ------------------------------
          SUBROUTINE FJ (N,X,Y,PD)
          IMPLICIT REAL*8 (A-H),REAL*8 (O-Z)
          DIMENSION Y(N),PD(N,N)
          RETURN
          END
          SUBROUTINE EQCNST (TEMP,EQ,A,B)
          IMPLICIT REAL*8 (A-H), REAL*8 (O-Z)
          DIMENSION EQ(8)
          ATEMP=TEMP-298.15D0
          A=.4919D0+7.143D-4*ATEMP+2.113D-6*ATEMP**2+1.172D-8*ATEMP**3
          B=.3249D0+2.099D-4*ATEMP-2.582D-6*ATEMP**2+2.589D-8*ATEMP**3
"
"         CALCULATE EQUILIBRIUM CONSTANTS
"
          EQ(1)=0.D0
          EQ(2)=DEXP(33.334D0-7629.9D0/TEMP)
          EQ(3)=0.D0
"         IF(TEMP.LE.325.15D0)EQ(4)=DEXP(19.804D0-3140.0D0/TEMP)
"         IF(TEMP.GT.325.15D0)EQ(4)=DEXP(34.182D0-7815.2D0/TEMP)
          EQ(4)=DEXP(-900.421D0+39110.926D0/TEMP+136.626D0*DLOG(TEMP))
          EQ(6)=10.D0**(3.339D0-337.37D0/TEMP)
          EQ(7)=DEXP(30.692D0-7290.4D0/TEMP)
          EQ(8)=10.D0**2.38D0*DEXP(-754.8D0/TEMP+2.333D0)
          RETURN
          END
          SUBROUTINE SPLINE (XTC,TC,Y,C,MO)
          IMPLICIT REAL*8 (A-H), REAL*8 (O-Z)
          REAL*8 Y(101),C(100,3),EXTENT(101),REDOX(101),XTC(5),TC(5)
          REAL*8 MO,WK(606),K(10)
          COMMON TEMP
          VOL=1.D0
          EXTENT(1)=0.0D0
          CALL EQUIL(XTC,K,T,EDIFF,1)
          REDOX(1)=E
          DO 200 J2=2,101
          EXTENT(J2)=EXTENT(J2-1)+0.0100D0*MO
```

```
      TC(1)=XTC(1)-2.59D0*EXTENT(J2)/VOL
      TC(2)=XTC(2)+2.83D0*EXTENT(J2)/VOL
      TC(5)=XTC(5)+EXTENT(J2)/VOL
      IF (TC(1).LT.1.D-6) TC(1)=DABS(1.D-6)
      CALL EQUIL(TC,K,E,EDIFF,2)
200   REDOX(J2)=E
      IJOB=2
      CALL ICSSCV (%XTENT,REDOX,101,Y,C,100,IJOB,WK,IER)
"     DO 201 J3=1,1J1
"201   WRITE(13,*)EXTENT(J3),REDOX(J3),Y(J3)
      RETURN
      END
```

K.6 SUBROUTINE EQUIL(TC,C,E,EDIFF,N)

```
"     PROGRAM TO EVALUATE THE EQUILIBRIUM CONDITIONS OF A SOLUTION
"     GIVEN THE TOTAL SPECIES CONCENTRATION AND THE EQUILIBRIUM
"     CONSTANTS. THE PROGRAM ALSO ACCOUNTS FOR THE ACTVTY COEFFS
"     NOT BEING UNITY, AND THE DEBYE-HUCKEL EQUATION IS USED TO
"     CALCULATE THEM.
"     PROGRAM EQUIL
      IMPLICIT REAL*8 (A-H),REAL*8 (O-Z)
      DIMENSION DIAG(5),AA(10),BB(10),-
        BE(5),FF(5),Q(5,5),X(5),GA(5),-
        Y(10),G(5),CEQ(8),-
        TC(5),C(10),WKAREA(30)
      COMMON TEMP
      COMMON /HION/ PH
      COMMON /EQUILB/ EQ(8),A,B
      COMMON /EQOXLC/ Z(10),A0(10),OHM(10)
"
"     ASSUMING TOTAL DISSOCIATION CALCULATE IONIC STENGTH
"     AND SET INITIAL CONCENTRATION GUESS AT TOTAL DISSOCIATION
"     CONCENTRATIONS
"
      TC(4)=3.DG/2.D0*TC(1)+TC(2)+.5D0*TC(3)+TC(5)
        XIONS=0.
        DO 40 KO=1,5
          IF(N.GT.1)THEN
            C(KO)=C(KO)
          ELSE
         C(KO)=TC(KO)
         C(9)=C(3)/2.D0
        END IF
40      XIONS=XIONS+Z(KO)**2*C(KO)
        XIONS=XIONS/2.D0
        ITR=0
42    ITR=ITR+1
"
"       CALCULATE ACTIVITY COEFFS FROM DEBYE-HUCKEL EQUATION
"
```

```
      DO 45 KA=1,10
       Y(KA)=10.0D0**((-A*Z(KA)**2*XIONS**.5D0)/-
        (1+AD(KA)*B*XIONS**.5D0))
45    CONTINUE
C
C CALCULATE THE EQUILIBRIUM CONSTANTS IN TERMS OF CONCENTRATION
C
      CEQ(1)=EQ(1)*Y(1)*Y(3)*Y(4)**2
      CEQ(2)=EQ(2)*Y(1)*Y(3)*Y(4)/Y(6)
      CEQ(3)=EQ(3)*Y(1)*Y(4)**2/Y(7)
      CEQ(4)=EQ(4)*Y(1)*Y(4)/Y(8)
      CEQ(6)=EQ(6)*Y(2)*Y(4)
      CEQ(7)=EQ(7)*Y(2)*Y(3)*Y(4)/Y(10)
      CEQ(8)=EQ(8)*Y(5)*Y(4)
      CALL SULF(TEMP,XIONS,AEQ,C)
      CEQ(5)=AEQ
C
C     GENERATE MATRIX AND VECTOR FOR THE SOLUTION OF THE
C     NON-LINEAR EQUATIONS BY A NEWTON-RAPHSON TECHNIQUE
C     CALCULATE VECTOR G
C
      CALL GG(C,TC,G,CEQ)
      DO 50 KB=1,5
       GA(KB)=G(KB)
50     G(KB)=-G(KB)
C
C     CALCULATE MATRIX Q
C
      Q(1,1)=1+CEQ(1)*C(3)*C(4)**2+CEQ(2)*C(3)*C(4)+CEQ(3)-
        *C(4)**2+CEQ(4)*C(4)
      Q(1,2)=0.D0
      Q(1,3)=CEQ(1)*C(1)*C(4)**2+CEQ(2)*C(1)*C(4)
      Q(1,4)=2*CEQ(1)*C(1)*C(3)*C(4)+CEQ(2)*C(1)*C(3)+2-
        *CEQ(3)*C(1)*C(4)+CEQ(4)*C(1)
      Q(1,5)=0.D0
      Q(2,1)=0.D0
      Q(2,2)=1+CEQ(6)*C(4)+CEQ(7)*C(3)*C(4)
      Q(2,3)=CEQ(7)*C(2)*C(4)
      Q(2,4)=CEQ(6)*C(2)+CEQ(7)*C(2)*C(3)
      Q(2,5)=0.D0
      Q(3,1)=CEQ(1)*C(3)*C(4)**2+CEQ(2)*C(3)*C(4)
      Q(3,2)=CEQ(7)*C(3)*C(4)
      Q(3,3)=1+CEQ(1)*C(1)*C(4)**2+CEQ(2)*C(1)*C(4)+-
        CEQ(5)*C(4)+CEQ(7)*C(2)*C(4)
      Q(3,4)=2*CEQ(1)*C(1)*C(3)*C(4)+CEQ(2)*C(1)*C(3)+-
        CEQ(5)*C(3)+CEQ(7)*C(2)*C(3)
      Q(3,5)=0.D0
      Q(4,1)=2*CEQ(1)*C(3)*C(4)**2+CEQ(2)*C(3)*C(4)+-
        2*CEQ(3)*C(4)**2+CEQ(4)*C(4)
      Q(4,2)=CEQ(6)*C(4)+CEQ(7)*C(3)*C(4)
      Q(4,3)=2*CEQ(1)*C(1)*C(4)**2+CEQ(2)*C(1)*C(4)+-
        CEQ(5)*C(4)+CEQ(7)*C(2)*C(4)
      Q(4,4)=1+4*CEQ(1)*C(1)*C(3)*C(4)+CEQ(2)*...1)*C(3)+-
        4*CEQ(3)*C(1)*C(4)+CEQ(4)*C(1)+CEQ(5)*C(3)+-
```

```
        CEQ(6)*C(2)
      Q(4,4)=Q(4,4)+CEQ(7)*C(2)*C(3)+CEQ(8)*C(5)
      Q(4,5)=CEQ(8)*C(4)
      Q(5,1)=0.D0
      Q(5,2)=0.D0
      Q(5,3)=0.D0
      Q(5,4)=CEQ(8)*C(5)
      Q(5,5)=1+CEQ(8)*C(4)
C
C     RE-ARRANGING Q IN TERMS OF FRACTIONAL SHIFTS
C
      DO 65 KCA=1,5
        DO 55 KCB=1,5
          Q(KCA,KCB)=Q(KCA,KCB)*C(KCB)
55      CONTINUE
        DIAG(KCA)=Q(KCA,KCA)
        IF(TC(KCA).LE.0)DIAG(KCA)=1.0D0
65    CONTINUE
C
C     MATRIX SCALING
C
      TOTAL=0.0D0
      DO 75 KAC=1,5
        G(KAC)=G(KAC)/(DIAG(KAC)**.5D0)
        DO 70 KAD=1,5
          Q(KAC,KAD)=Q(KAC,KAD)/((DIAG(KAC)*DIAG(KAD))**.5DG)
          TOTAL=TOTAL+Q(KAC,KAD)**2
70      CONTINUE
75    CONTINUE
C
C     CALCULATE THE INVERSE OF THE MATRIX AND CHECK FOR
C     SINGULARITY USING THE DETERMINANT CRITERION
C
      CALL LRQT1F(Q,1,5,5,G,1,WKAREA,IER)
      IF(IER.EQ.129)GO TO 170
C
C     CALCULATE THE FRACTIONAL SHIFTS, VECTOR X
C
      DO 80 KE=1,5
        X(KE)=G(KE)/DIAG(KE)**.5D0
        IF(X(KE).GT.1.0D0)X(KE)=0.95D0
        IF(X(KE).LT.-1.0D0)X(KE)=-0.95D0
80    CONTINUE
C
C     CALCULATION OF ALPHA_MAX
C
C     SSHIFT=X(1)
C     DO 90 KF=1,5
C       IF(X(KF).LT.SSHIFT)SSHIFT=X(KF)
C90    CONTINUE
C     ALFAMX=-.95/SSHIFT
C     THI0=0.
C     THI1=0.
C     THI05=0.
```

```
"       IF(ALFAMX.GT.1.0)ALFAMX=1.0
"       DO 150 KK=1,5
"         AA(KK)=C(KK)*(1.+ALFAMX*X(KK))
"         BB(KK)=C(KK)*(1.+.5*ALFAMX*X(KK))
"150     CONTINUE
"       CALL GG(AA,TC,FF,CEQ)
"       CALL GG(BB,TC,EE,CEQ)
"       DO 155 KL=1,5
"         THI0=THI0+DABS(GA(KL))**2
"         THI1=THI1+DABS(FF(KL))**2
"         THI05=THI05+DABS(EE(KL))**2
"155     CONTINUE
"      ALFAMN=.5*ALFAMX*(4.*THI05-3.*THI0-THI1)/(2.*THI05-THI0-THI1)
"
"       NEXT ITR OF CONCENTRATION CALCULATION
"
       ALFAMN=1.0D0
       NERROR=0
       DO 160 KM=1,5
         C(KM)=C(KM)*(1.D0+ALFAMN*X(KM))
         IF(C(KM).LT.0.0)C(KM)=1.D-5
         IF(DABS(ALFAMN*X(KM)).GT.0.0001D0) NERROR=NERROR+1
160    CONTINUE
"
"      CALCULATION OF CONCENTRATIONS C(6) TO C(10)
"
       C(6)=CEQ(2)*C(1)*C(3)*C(4)
       C(7)=CEQ(3)*C(1)*C(4)**2
       C(8)=CEQ(4)*C(1)*C(4)
       C(9)=CEQ(5)*C(3)*C(4)
       C(10)=CEQ(7)*C(2)*C(3)*C(4)
       XIONS=0.0D0
       DO 165 KP=1,10
         XIONS=XIONS+Z(KP)**2*C(KP)
165    CONTINUE
       XIONS=XIONS/2.D0
       IF(NERROR.GT.0)GO TO 42
         E=771.0D0+1.19D0*(TEMP-298.15D0)+8.6158D-5*TEMP*-
          (DLOG(C(1)*Y(1)/C(2)/Y(2)))*1000.D0
"          0.5D0*DLOG(C(5)*Y(5)))*1000D0
       SLIZI=0.D0
       SLIMI=0.D0
       DO 167 KQ=1,10
         SLIMI=SLIMI+OHM(KQ)*C(KQ)
167      SLIZI=SLIZI+OHM(KQ)*C(KQ)/Z(KQ)
       SLIZI=SLIZI-2.D0*(OHM(7)*C(7)+OHM(9)*C(9))
       EDIFF=8.6155D-2*TEMP*(SLIZI+9.975)/(SLIMI-524.475)*-
          DLOG(SLIMI/524.475)
"      E=506.1D0+8.6158D-5*TEMP/2*-
"        DLOG((C(1)*Y(1))**2/(C(2)*Y(2))**2/(C(5)*Y(5)))*1000
       PH=E
       GO TO 175
170    WRITE(12,171)
171    FORMAT(5X,'MATRIX SINGULAR')
```

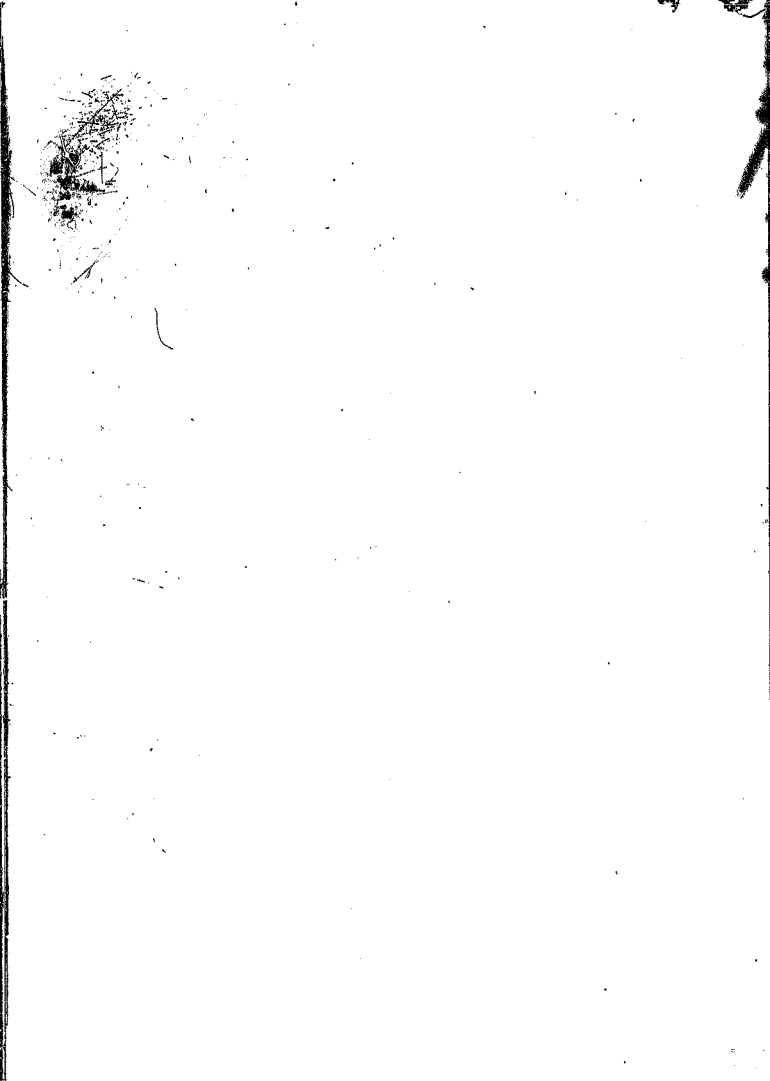

Author Crundwell Frank Kenneth
Name of thesis Kinetics Of The Leaching Of Sphalerite In Acidic Ferric Sulphate Media In The Presence And Absence Of Oxygen. 1985

PUBLISHER:
University of the Witwatersrand, Johannesburg
©2013

LEGAL NOTICES:

Copyright Notice: All materials on the University of the Witwatersrand, Johannesburg Library website are protected by South African copyright law and may not be distributed, transmitted, displayed, or otherwise published in any format, without the prior written permission of the copyright owner.

Disclaimer and Terms of Use: Provided that you maintain all copyright and other notices contained therein, you may download material (one machine readable copy and one print copy per page) for your personal and/or educational non-commercial use only.

The University of the Witwatersrand, Johannesburg, is not responsible for any errors or omissions and excludes any and all liability for any errors in or omissions from the information on the Library website.